Supporting information

Curved graphene nanoribbons derived from tetrahydropyrene-based polyphenylenes via one-pot K-region oxidation and Scholl cyclization

Sebastian Obermann,[a] Wenhao Zheng,[b] Jason Melidonie,[a] Steffen Böckmann,[c] Silvio Osella,[d] Nicolás Arisnabarreta,[e] L. Andrés Guerrero León,[a] Felix Hennersdorf,[f] David Beljonne,[g] Jan J. Weigand,[f] Mischa Bonn,[b] Steven De Feyter,[e] Michael Ryan Hansen,[c] Hai I. Wang,[b] Ji Ma,[a,h,*] Xinliang Feng[a,h,*]

[a] Center for Advancing Electronics Dresden (cfaed) & Faculty of Chemistry and Food Chemistry, Technische Universität Dresden, D-01069 Dresden, Germany

[b] Max-Planck-Institute for Polymer Research, D-55128 Mainz, Germany

[c] Institute of Physical Chemistry, Westfälische Wilhelms-Universität (WWU) Münster, D-48149 Münster, Germany

[d] Chemical and Biological Systems Simulation Lab Centre of New Technologies University of Warsaw Banacha 2C, Warsaw 02–097, Poland

[e] Department of Chemistry, Division of Molecular Imaging and Photonics, KU Leuven, Celestijnenlaan 200F, 3001 Leuven, Belgium

[f] Chair of Inorganic Molecular Chemistry, Technische Universität Dresden, Dresden, Germany

[g] Laboratory for Chemistry of Novel Materials, Materials Research Institute, University of Mons, Mons 7000, Belgium

[h] Max Planck Institute of Microstructure Physics, Weinberg 2, 06120 Halle, Germany

Table of Contents

1 Experimental section

1.1 General methods and materials

All the reagents were obtained from Sigma Aldrich, TCI, abcr, Alfa Aesar, Strem, fluorochem, and chempur. All these chemicals were used as received without further purification. All reactions dealing with air- or moisture-sensitive compounds were carried out in a dry reaction vessel under argon (Ar) atmosphere by using standard vacuum-line and Schlenk techniques. Anhydrous dichloromethane and tetrahydrofuran were obtained from MBRAUN MB-SPS-5 solvent purification system.

Thin layer chromatography (TLC) was performed on silica-coated aluminium sheets with a fluorescence indicator (TLC silica gel 60 F254, purchased from Merck KGaA).

Column chromatography was performed on silica (SiO_2, particle size 0.063 - 0.200 mm, purchased from VWR).

Nuclear magnetic resonance (NMR) spectra were recorded on Bruker AVANCE-II 300 and Bruker Avance III HD 300 spectrometers (300 MHz and 75.5 MHz for ^1H and ^{13}C respectively) and on a Bruker DRX 500 (500 MHz and 125.7 MHz for ^1H and ^{13}C respectively) using a 5 mm $^1H/^{13}C$ gradient probe at room temperature. $CDCl_3$ (δ (^{13}C) = 77.36 ppm) was used as solvent, lock and internal standard for ^{13}C measurements. The ^1H-spectra were referenced to the internal TMS-standard at δ (^1H) = 0.00 ppm. The 2D NMR spectra were recorded using the standard pulse sequences of the Bruker software package (TOPSPIN 3.6). The sample temperature was controlled by the Bruker variable temperature accessory BVT-3000.

The mass spectrometry analysis was performed on a Bruker Autoflex Speed MALDI-TOF MS (Bruker Daltonics, Bremen, Germany) using DCTB (*trans*-2-[3-(4-tert-Butylphenyl)-2-methyl-2-propenylidene]malononitrile) as matrix.

High-Resolution Atmospheric Pressure Chemical Ionization (APCI) mass spectra was recorded with Agilent 6538 Ultra High Definition (UHD) Accurate-Mass Q-TOF LC/MC system, using the positive mode.

UV-Visible spectra were measured on an Agilent Cary 5000 UV-Vis-NIR spectrophotometer by using 10 mm optical-path quartz cell at room temperature. Photoluminescence spectra were measured on PerkinElmer fluorescence spectrometer LS 55.

Recycling gel permeation chromatography (rGPC) was carried out on a Japan Analytical Industry JAI-HPLC LC 9110 II Next equipped with a JAIGEL-2HH and a JAIGEL-1HH column. Chloroform was used as the eluent in a flow rate of 5 mL/min.

Relative molar masses were determined by gel permeation chromatography (GPC) with an Aligent Technologies 1260 Infinity LC system equipped with two Resipore columns and RI and UV–Vis detection. Chloroform was used as an eluent with a flow rate of 1 mL min^{-1}. The measurements were carried out at 40 ºC. The molar masses were calculated relative to polystyrene standards with low dispersity.

The Raman spectra were recorded with a confocal Raman setup Monovista CRS+ from S&I Gmbh, using a 515 nm continuous-wave single-frequency diode pumped laser Cobolt Fandango^{TM} from Hübner Photonics. The laser beam was focussed onto the sample using a 20x Nikon objective, with laser powers of approx. 0.35 mW on the sample. Exposure times for single spectra were 5 s with 20 accumulations.

1.2 Synthetic procedures and characterization data

1.2.1 4,5,9,10-tetrahydropyrene (3)
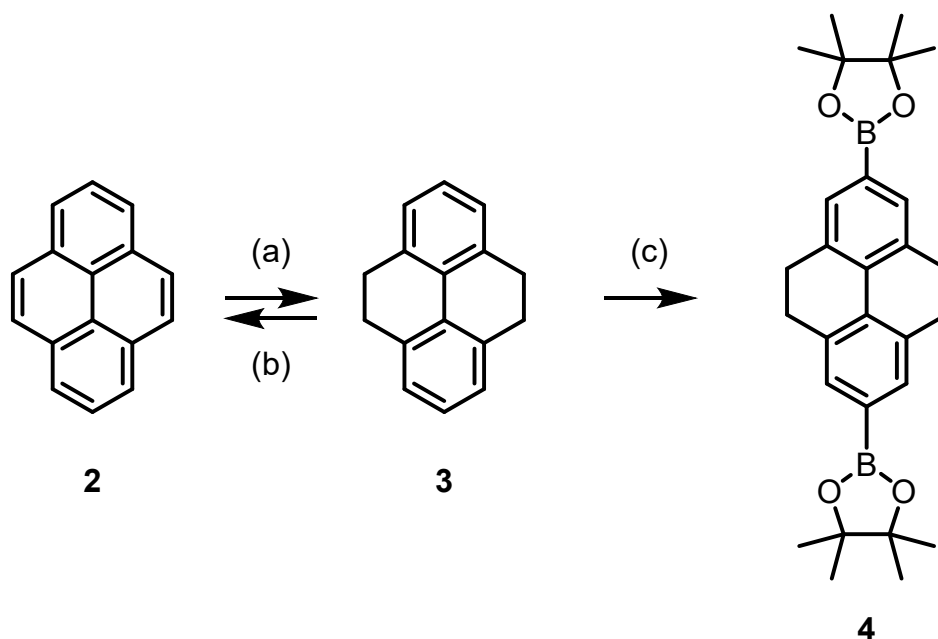
Scheme S1. Synthetic route to boronic ester **4**. (a) Raney-Ni, EtOAc, rt, 2d, then 20 bar H_2, Pd/C (10%), 60 °C, 1 d, 31%. (b) $FeCl_3$, DCM/MeNO$_2$, rt, 5 min, 53%. (c) (BPin)$_2$, 4,4'-di-tBu-2,2'-bipyridine, (Ir(OMe)(COD))$_2$, THF, 80 °C, overnight, 73%.
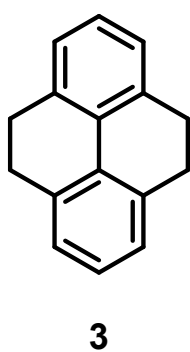

A 250 mL round bottle flask was charged with pyrene (10 g, 49.44 mmol), Raney-Nickel slurry (~5 g) and ethyl acetate (150 mL). The mixture was stirred for 48 hours at room temperature to achieve desulfurization. The mixture was filtrated, degassed by flushing with argon for 15 minutes and transferred to a 400 mL autoclave. Palladium on charcoal (10%, 2.63 g, 2.47 mmol) was added to the autoclave. After purging the autoclave three times with argon and twice with hydrogen, the autoclave was pressurized to 20 bar and heated to 60 °C. After 24 hours of reaction time, the catalyst was filtered off and column chromatography was carried out in isohexane. 4,5,9,10-tetrahydropyrene was obtained as a colorless solid in 31% yield (3.20 g, 15.51 mmol). The analysis agrees with reported results.[1]

^{1}H NMR (300 MHz, CDCl$_3$) δ 7.09 – 6.90 (m, 6H), 2.78 (s, 8H).

^{13}C NMR (75 MHz, CDCl$_3$) δ 135.71, 130.94, 127.37, 126.26, 28.65.

HR-MS (APCI): calc. m/Z =206.10955, exp. m/Z = 206.10895, error = -2.91 ppm.

1.2.2 Pyrene (2)
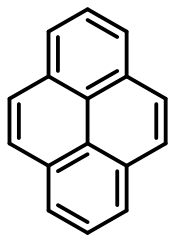
2

To a 25 mL dried Schlenk flask, 4,5,9,10-tetrahydropyrene (25 mg, 0.12 mmol) were added. The starting material was dissolved in 20 mL of dry dichloromethane. A suspension of $FeCl_3$ (197 mg, 1.21 mmol) in $MeNO_2$ (2 mL) was prepared and both mixtures were purged with argon for 20 minutes. The $FeCl_3$-suspension was added to the reaction flask dropwise at room temperature. After 5 minutes, water was added, and the mixture was extracted with dichloromethane three times. The combined organic layers were dried over $MgSO_4$. The crude product was adsorbed on silica gel and a flash column chromatography was carried out with hexane as the eluent. Pyrene (**2**) was obtained as a yellowish solid in 53% yield (13 mg, 0.06 mmol).[2]

^{1}H NMR (300 MHz, CDCl$_3$) δ 8.12 (d, J = 7.6 Hz, 4H), 8.01 (s, 4H), 7.98 – 7.90 (m, 2H).

^{13}C NMR (75 MHz, CDCl$_3$) δ 131.49, 127.73, 126.20, 125.29, 123.77.

HR-MS (APCI): calc. m/Z =202.07825, exp. m/Z = 202.07806, error = -0.92 ppm.

1.2.3 2,7-bis(4,4,5,5-tetramethyl-1,3,2-dioxaborolan-2-yl)-4,5,9,10-tetrahydropyrene (4)
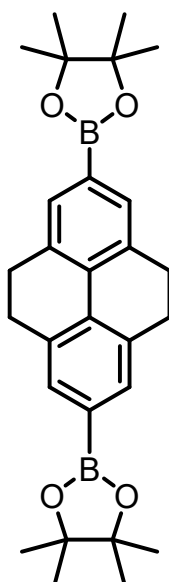

4

A flame-dried 50 mL Schlenk tube was charged under argon with 4,5,9,10-tetrahydropyrene (500 mg, 2.42 mmol), 4,4,4',4',5,5,5',5'-octamethyl-2,2'-bi(1,3,2-dioxaborolane) (1.35 g, 5.33 mmol), 4,4'-di-tert-butyl-2,2'-bipyridine (20 mg, 0.07 mmol) and (Ir(OMe)(COD))$_2$ (16 mg, 0.02 mmol). The flask was evacuated and flushed with argon three times. Dry THF (25 mL) was added, the flask was sealed and heated to 80 °C overnight. The reaction mixture was directly adsorbed on silica gel and column chromatography was carried out using 10% to 50% dichloromethane in isohexane. The final product was isolated as a colorless solid in 73% yield (808 mg, 1.76 mmol).

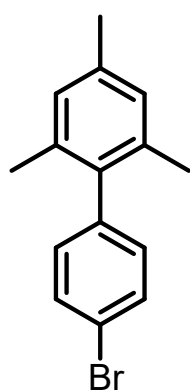^{1}H NMR (300 MHz, CDCl$_3$) δ 7.40 (s, 4H), 2.79 (s, 8H), 1.25 (s, 24H).

^{13}C NMR (75 MHz, CDCl$_3$) δ 135.40, 133.60, 132.63, 84.06, 83.81, 28.37, 25.34, 25.18.

HR-MS (APCI): calc. m/Z =458.27997, exp. m/Z = 458.27996, error = -0.02 ppm.

1.2.4 4'-Bromo-2,4,6-trimethyl-1,1'-biphenyl (I)
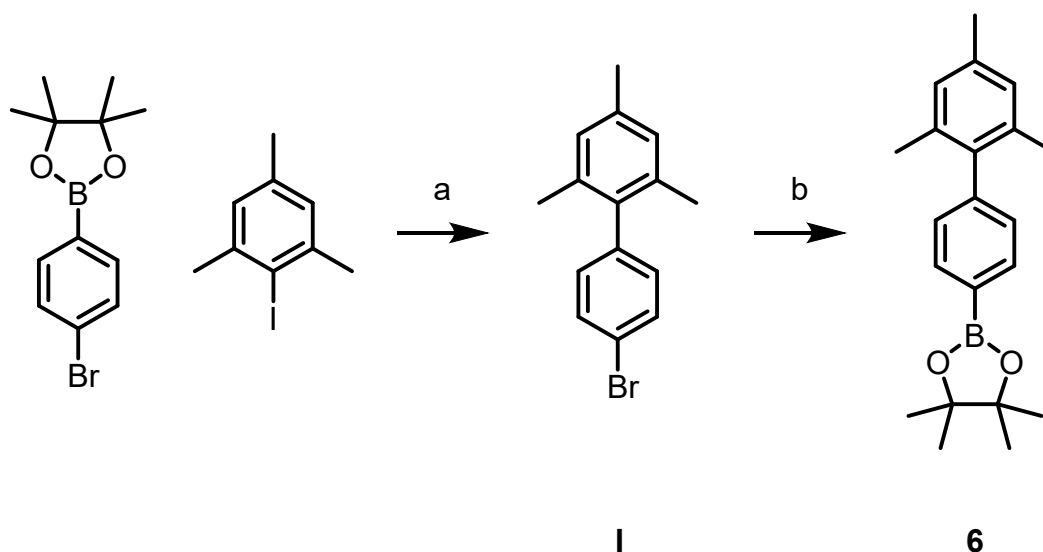
Scheme S2. Synthetic route to boronic ester **6**. (a) Pd(PPh₃)₄, Na₂CO₃, H₂O, EtOH, DME, 24 h, 90 °C, 70%. (b) Pd(dppf)Cl₂ • DCM, KOAc, (BPin)₂, DME, 24 h, 90 °C, 83%.


A 500 mL round bottom flask was charged with 4-bromophenylboronic acid (2.05 g, 10.21 mmol), 2-iodomesitylene (3.01 g, 12.25 mmol) and Na₂CO₃ (5.41 g, 51.04 mmol). Water (20 mL), EtOH (4 mL) and DME (50 mL) were added and the mixture was purged with Argon for 20 minutes. Pd(PPh₃)₄ (590 mg, 510 µmol) was added. The flask has been equipped with a reflux condenser and the mixture was stirred for 24 h at 90 °C. After cooling to room temperature, the mixture was washed with water and the aqueous layer was extracted three times with DCM. The combined organic layers were dried with MgSO₄, filtrated, and evaporated in vacuo. Column chromatography in hexane yielded the title compound as a colorless solid in 70% yield (1.96 g, 7.12 mmol).

¹H NMR (300 MHz, CDCl₃) δ 7.48 – 7.41 (m, 2H), 6.98 – 6.89 (m, 2H), 6.85 (s, 2H), 2.23 (s, 3H), 1.90 (s, 6H).

¹³C NMR (76 MHz, CDCl₃) δ 140.32, 138.01, 137.25, 136.09, 131.90, 131.44, 128.47, 120.93, 21.31, 21.00.

HR-MS (APCI): calc. m/Z =274.03571, exp. m/Z = 274.03609, error = +1.37 ppm.

1.2.5 4,4,5,5-tetramethyl-2-(2',4',6'-trimethyl-[1,1'-biphenyl]-4-yl)-1,3,2-dioxaborolane (6)
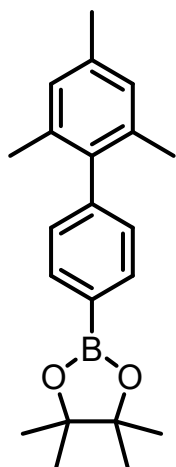
6

To a 500 mL round bottom flask, 4'-bromo-2,4,6-trimethyl-1,1'-biphenyl (**I**, 6.96 g, 25.29 mmol), potassium acetate (19.86 g, 202.33 mmol), 4,4,4',4',5,5,5',5'-octamethyl-2,2'-bi(1,3,2-dioxaborolane) (25.69 g, 101.17 mmol) and Pd(dppf)Cl$_2$ • CH$_2$Cl$_2$ (2.07 g, 2.53 mmol) were added. The solids were evacuated and flushed with argon three times. Then, 230 mL of dimethoxyethane were added and the mixture was degassed under stirring by flushing with argon gas for 30 minutes. Afterwards, the reaction was brought to reflux and was allowed to stir overnight. After cooling to room temperature, the organic layer was washed with water and the aqueous layer was then extracted with DCM twice. The combined organic layers were dried by MgSO$_4$ and the crude product was purified by column chromatography (1:1 iso-hexane/dichloromethane) to afford a yellowish solid. Final purification was achieved by recrystallization in methanol to yield colorless crystals in 83% yield (6.76 g, 20.98 mmol).

^{1}H NMR (300 MHz, CDCl$_3$) δ 7.79 (d, *J* = 8.1 Hz, 2H), 7.08 (d, *J* = 8.1 Hz, 2H), 6.85 (s, 2H), 2.24 (s, 3H), 1.91 (s, 6H), 1.29 (s, 12H).

^{13}C NMR (76 MHz, CDCl$_3$) δ 144.60, 139.27, 136.94, 136.05, 135.17, 129.12, 128.39, 84.11, 25.27, 25.21, 21.35, 21.02.

HR-MS (APCI): calc. m/Z =322.21041, exp. m/Z = 322.2105, error = +0.28 ppm.

1.2.6 1,2,3-tribromo-5-nitrobenzene (5)
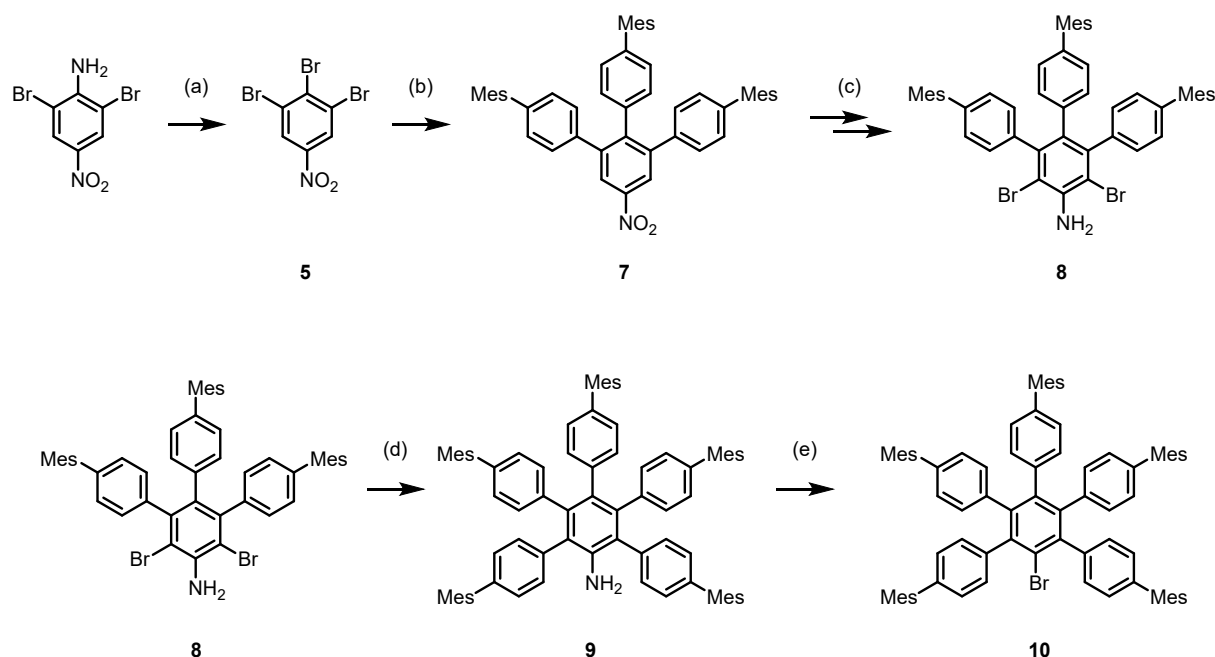
Scheme S3. Synthetic route to building block **10**. (a) H_2O/HBr, NaNO$_2$, -15 °C to 35 °C, overnight, urea, CuBr, HBr, 0 °C to reflux, 55%. (b) **6**, Pd(dppf)Cl$_2$ • CH$_2$Cl$_2$, K$_3$PO$_4$, H$_2$O, PhMe, 24 h, 115 °C, 69%. (c) SnCl$_2$, EtOH, EtOAc, reflux, overnight. Then NBS, CHCl$_3$, rt, 10 minutes, 60%. (d) **6**, Pd(dppf)Cl$_2$ • CH$_2$Cl$_2$, K$_3$PO$_4$, H$_2$O, PhMe, 115 °C, overnight, 77%. (e) isopentylnitrite, CHBr$_3$, 100 °C, overnight, 47%.
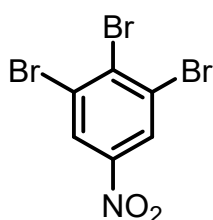
A 250 mL round bottom flask was charged with water (26 mL) and aq. HBr (26 mL). 2,6-dibromo-4-nitroaniline (10 g, 33.79 mmol) was added in portions under stirring. The flask was cooled by an ethylene glycol/dry ice mixture and NaNO$_2$ (3.50 g, 50.69 mmol) in 20.5 mL of water was added via a syringe pump over 30 minutes. The mixture was then stirred overnight at 35 °C. After cooling to room temperature, 1.52 g (25.34 mmol) of urea were added to the mixture and it was allowed to stir for another 20 minutes. A flask containing CuBr (7.27g, 50.69 mmol) and aq. HBr (30 mL) was cooled to 0 °C. The reaction mixture was poured into the CuBr/HBr mixture and stirred at rt for 2.5 hours and an additional 1.5 hours at reflux. After the mixture cooled down to room temperature, the yellow solid was filtered off. Column chromatography of 25% dichloromethane in isohexane yielded the target compound in 55% yield (6.70 g, 18.62 mmol).

^{1}H NMR (500 MHz, CDCl$_3$) δ 8.36 (s, 1H).

^{13}C NMR (126 MHz, CDCl$_3$) δ 147.10, 136.06, 127.30, 127.12.

HR-MS (APCI): calc. m/Z =356.76357, exp. m/Z = 356.76205, error = -4.26 ppm.

1.2.7 Compound 7

7
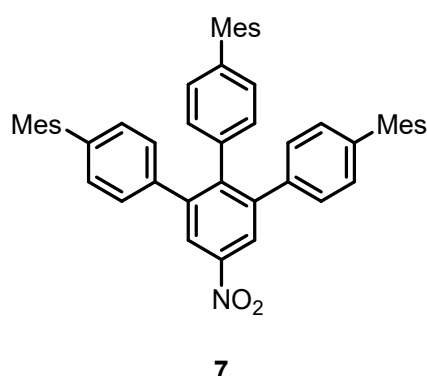
A 250 mL Schlenk flask was charged with 1,2,3-tribromo-5-nitrobenzene (800 mg, 2.22 mmol), boronic ester **6** (2.87 g, 8.89 mmol), potassium phosphate (2.83 g, 13.34 mmol) and Pd(dppf)Cl$_2$ • CH$_2$Cl$_2$ (325 mg, 0.44 mmol). The flask was evacuated and flushed by argon three times. Afterwards, toluene (36 mL) and water (4 mL) were added and the mixture was degassed by flus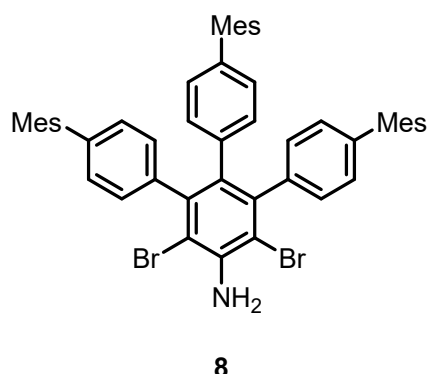hing with argon for 30 minutes. The flask was sealed and heated to 115 °C overnight. After cooling to room temperature, dichloromethane and water were added and the aqueous layer was extracted three times with dichloromethane. After drying with MgSO$_4$ and filtration, column chromatography was carried out in a solvent mixture of 50% dichloromethane in isohexane. The product was isolated as a yellowish solid in 69% yield (1.08 g, 1.53 mmol).

^{1}H NMR (300 MHz, CDCl$_3$) δ 8.34 (s, 2H), 7.12 (d, *J* = 8.2 Hz, 4H), 6.98 – 6.76 (m, 12H), 6.72 (d, *J* = 8.1 Hz, 2H), 2.24 (s, 6H), 2.21 (s, 3H), 1.86 (s, 12H), 1.75 (s, 6H).

^{13}C NMR (75 MHz, CDCl$_3$) δ 147.27, 146.22, 143.90, 140.49, 140.14, 138.81, 138.75, 138.47, 137.06, 137.02, 136.69, 136.17, 135.96, 131.71, 130.25, 129.18, 128.69, 128.36, 128.24, 124.22, 21.35, 21.33, 20.91, 20.67.

HR-MS (APCI): calc. m/Z =705.36068, exp. m/Z = 705.36057, error = -0.15 ppm.

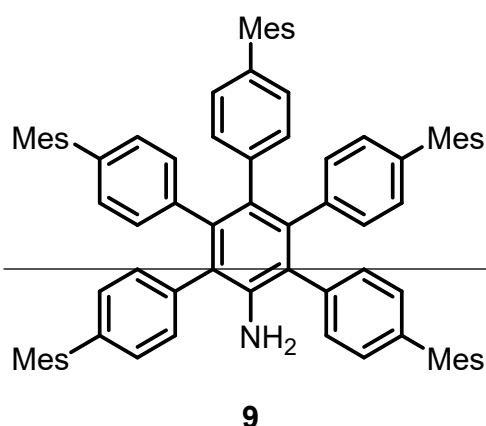### 1.2.8 Compound 8

Mes

Mes

Mes

Br

Br

NH₂

8

A 250 mL Schlenk flask was charged with compound **7** (1.03 g, 1.45 mmol) and $SnCl_2$ (1.43 g, 7.56 mmol). After evacuating and flushing three times with argon, ethanol (25 mL) and ethyl acetate (25 mL) were added and the mixture was brought to reflux overnight. After cooling to room temperature, the mixture was poured into an ice/water mixture (200 mL) and NaOH pellets were slowly added until the pH was basic. The mixture was transferred to a separating funnel, dichloromethane was added and the aqueous layer was extracted three times by dichloromethane. After drying by $MgSO_4$, all volatiles were evaporated and the remaining beige solid was transferred to a 100 mL round bottom flask and dissolved in chloroform (30 mL). NBS (0.52 g, 2.9 mmol) was added to the solution and the dark red mixture was stirred for 10 minutes at room temperature. After TLC indicated full conversion, the mixture was transferred to a separating funnel, saturated thiosulfate solution was added and the aqueous layer was extracted three times with dichloromethane. After drying with $MgSO_4$, the crude product was purified by silica gel column chromatography with an eluent of 33% dichloromethane in isohexane. The product was isolated as a beige powder in 60% yield (0.73 g, 0.87 mmol) over two steps.

^1H NMR (500 MHz, $CDCl_3$) δ 7.05 (d, J = 8.1 Hz, 4H), 6.87 (d, J = 8.1 Hz, 4H), 6.84 (s, 2H), 6.80 (s, 2H), 6.76 – 6.72 (m, 4H), 6.53 (d, J = 8.1 Hz, 2H), 2.23 (s, 6H), 2.19 (s, 3H), 1.94 (s, 6H), 1.71 (s, 6H), 1.63 (s, 6H).

^{13}C NMR (126 MHz, $CDCl_3$) δ 142.39, 142.03, 139.83, 139.57, 136.79, 136.63, 136.35, 136.15, 136.13, 133.13, 131.94, 130.69, 128.67, 128.26, 128.19, 128.06, 127.91, 110.60, 21.36, 21.31, 21.00, 20.85, 20.71.

HR-MS (APCI): calc. m/Z =675.3865, exp. m/Z = 675.38654, error = +0.06 ppm.

Mes

Mes

Mes

Mes

Mes

NH₂

Mes

9

1.2.9 Compound 9

A 50 mL Schlenk tube was charged with compound **8** (585 mg, 0.70 mmol), boronic ester **6** (565 mg, 1.75 mmol), potassium phosphate

(596 mg, 2.81 mmol) and Pd(dppf)Cl$_2$ (103 mg, 0.14 mmol). After addition of toluene (24 mL) and water (2.4 mL), the mixture was degassed by flushing with argon for 30 minutes. The vessel was then heated to 115 °C and was allowed to stir for 48 hours. After cooling to room temperature, water and dichloromethane were added and the aqueous layer was extracted three times by dichloromethane. After drying with MgSO$_4$, silica gel column chromatography in 1:1 dichloromethane/isohexane afforded the beige target compound in 77% yield (574 mg, 0.54 mmol).

^{1}H NMR (500 MHz, CDCl$_3$) δ 7.29 (d, *J* = 8.0 Hz, 4H), 6.97 (d, *J* = 8.0 Hz, 4H), 6.93 (d, *J* = 8.1 Hz, 4H), 6.87 – 6.83 (m, 6H), 6.77 (d, *J* = 6.8 Hz, 6H), 6.59 (d, *J* = 8.1 Hz, 4H), 6.54 (d, *J* = 8.1 Hz, 2H), 3.81 (s, 2H), 2.25 (s, 6H), 2.22 – 2.19 (m, 9H), 1.91 (s, 6H), 1.79 (s, 6H), 1.72 – 1.67 (m, 18H).

^{13}C NMR (126 MHz, CDCl$_3$) δ 141.51, 141.12, 139.75, 139.67, 139.57, 139.53, 139.44, 139.13, 138.19, 137.70, 137.18, 136.86, 136.55, 136.47, 136.31, 136.23, 136.20, 132.76, 132.01, 131.71, 131.37, 129.66, 128.31, 128.26, 128.06, 128.02, 128.00, 127.75, 127.66, 126.82, 21.36, 21.33, 21.04, 20.89, 20.77, 20.75.

HR-MS (APCI): calc. m/Z =1063.60560, exp. m/Z = 1063.60556, error = -0.04 ppm.

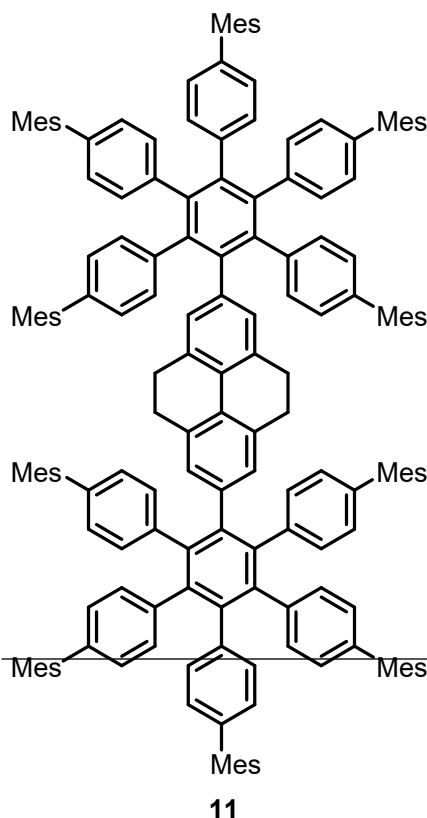### 1.2.10 Compound 10

Mes

Mes ... Mes

Br

Mes ... Mes

10
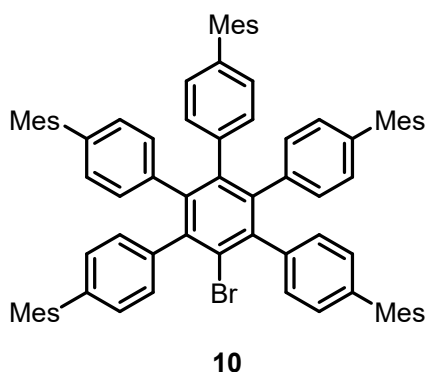
A dried 25 mL Schlenk tube was charged with compound **9** (270 mg, 0.25 mmol) and evacuated and argon flushed three times. Afterwards, bromoform (10 mL) was added and isoamylnitrite (68 µL, 0.51 mmol) was added via a Hamilton-syringe. The vessel was sealed and heated to 100 °C overnight. Water and dichloromethane were added, the aqueous layer was extracted three times with dichloromethane and the organic layer was dried using MgSO$_4$. Silica gel column chromatography with 25% dichloromethane in isohexane afforded the colorless solid **10** in 47% yield (134 mg, 0.12 mmol).

^{1}H NMR (500 MHz, CDCl$_3$) δ 7.21 (d, J = 8.1 Hz, 4H), 6.93 – 6.89 (m, 8H), 6.88 – 6.84 (m, 4H), 6.82 (s, 2H), 6.79 – 6.75 (m, 6H), 6.60 (d, J = 8.1 Hz, 4H), 6.57 (d, J = 8.1 Hz, 2H), 2.24 (s, 6H), 2.21 (s, 6H), 2.20 (s, 3H), 1.95 (s, 6H), 1.78 (s, 6H), 1.71 – 1.65 (m, 18H).

^{13}C NMR (126 MHz, CDCl$_3$) δ 142.43, 142.23, 140.86, 140.36, 139.61, 139.29, 139.19, 139.16, 138.96, 138.74, 138.67, 138.53, 136.73, 136.65, 136.45, 136.18, 136.14, 132.00, 131.80, 131.09, 128.59, 128.28, 128.18, 128.09, 127.97, 21.37, 21.33, 20.99, 20.92, 20.75.

HR-MS (APCI): calc. m/Z = 1126.50522, exp. m/Z = 1126.50524, error = +0.02 ppm.

1.2.11 Model compound precursor 11

A 10 mL Schlenk tube was charged with compound **4** (21 mg, 46 µmol), compound **10** (116 mg, 103 µmol) and potassium carbonate (38 mg, 275 µmol). The tube was evacuated and flushed with argon three times. Afterwards, toluene (2 mL) and water (0.5 mL) were added and the mixture was flushed with argon for 15 minutes. Pd(PPh$_3$)$_4$ (5 mg, 4.5 µmol) was added and the flask was sealed and heated to 115 °C for 48 hours. After cooling to room temperature, water and dichloromethane were added, the aqueous layer

11

was extracted three times by dichloromethane and the combined organic layers were dried over MgSO$_4$. Silica gel column chromatography with 25% to 50% dichloromethane in isohexane afforded the product as a colorless solid in 35% yield (37 mg, 16 μmol).

^{1}H NMR (300 MHz, CDCl$_3$) δ 6.95 – 6.86 (m, 10H), 6.80 – 6.73 (m, 8H), 6.63 – 6.54 (m, 10H), 6.47 (s, 2H), 6.36 (s, 2H), 2.21 (s, 13H), 2.10 (s, 6H), 1.77 – 1.67 (m, 24H), 1.53 (s, 6H).

^{13}C NMR (76 MHz, CDCl$_3$) δ 141.24, 140.83, 140.67, 140.43, 139.75, 139.67, 139.62, 139.47, 139.24, 139.17, 138.22, 138.18, 138.05, 136.57, 136.41, 136.36, 136.29, 136.24, 136.15, 135.76, 133.59, 132.37, 132.13, 129.67, 128.05, 127.84, 127.77, 21.34, 21.24, 20.75, 20.70.

HR-MS (MALDI-TOF): calc. m/Z = 2299.267, exp. m/Z = 2299.270, err.: +1.4 ppm.

1.2.12 Model compound 1

1
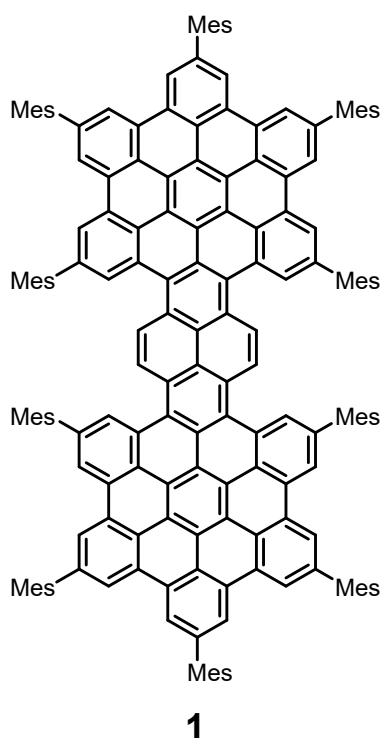
To a flame dried 10 mL Schlenk tube, compound **11** (10 mg, 4.4 μmol) and DDQ (21 mg, 92 μmol) were added. After evacuating and purging with argon three times, the solids were dissolved in dry and degassed dichloromethane (10 mL). Methanesulfonic acid (1 mL) was added at room temperature under stirring. The mixture was allowed to stir for 30 minutes at room temperature. Then, the initial amount of DDQ was added, together with 1 mL of trifluoromethanesulfonic acid. After three minutes of stirring at room temperature, the reaction was quenched with triethylamine, and water and dichloromethane was added. After extracting the aqueous layer three times with dichloromethane, the combined organic layers were dried over $MgSO_4$ and a silica gel column chromatography was carried out in 3:1 isohexane/dichloromethane to afford the bright red product in 60% yield (6 mg, 2.6 μmol).

^{1}H NMR (300 MHz, CDCl$_3$) δ 9.78 (s, 2H), 9.43 (s, 2H), 9.05 – 8.97 (m, 8H), 7.11 (s, 4H), 7.03 (s, 4H), 7.02 (s, 2H), 2.47 (s, 6H), 2.38 – 2.32 (m, 21H), 2.20 (s, 12H), 2.17 (s, 6H).

C NMR (^{13}C+HSQC, 75 MHz, CDCl$_3$) δ 139.19, 138.17, 138.13, 138.11, 138.06, 136.10, 136.04, 135.37, 135.12, 129.97, 127.61, 127.50, 127.41, 126.91, 123.47, 122.88, 122.79, 122.70, 122.64, 119.81, 20.51, 20.39, 20.36, 20.31, 20.16.

HR-MS (MALDI-TOF): calc. m/Z = 2271.048, exp. m/Z = 2271.058, err.: +4.4 ppm.

Remarks for the behavior of compound **11** under common Scholl reaction procedures: The use of triflic acid decomposed the starting material quickly. When using iron chloride, the desired target signal could be observed, but quickly reacted to an unknown side product 14 proton masses above the target mass. The formation of this side product could be suppressed to a large extent when carrying the reaction out at -40 °C, however, the oxidation of the K-regions was not complete under these

conditions (see Figure S3). In contrast, the described conditions in the manuscript yield compound **1** in a clean manner without any side products.
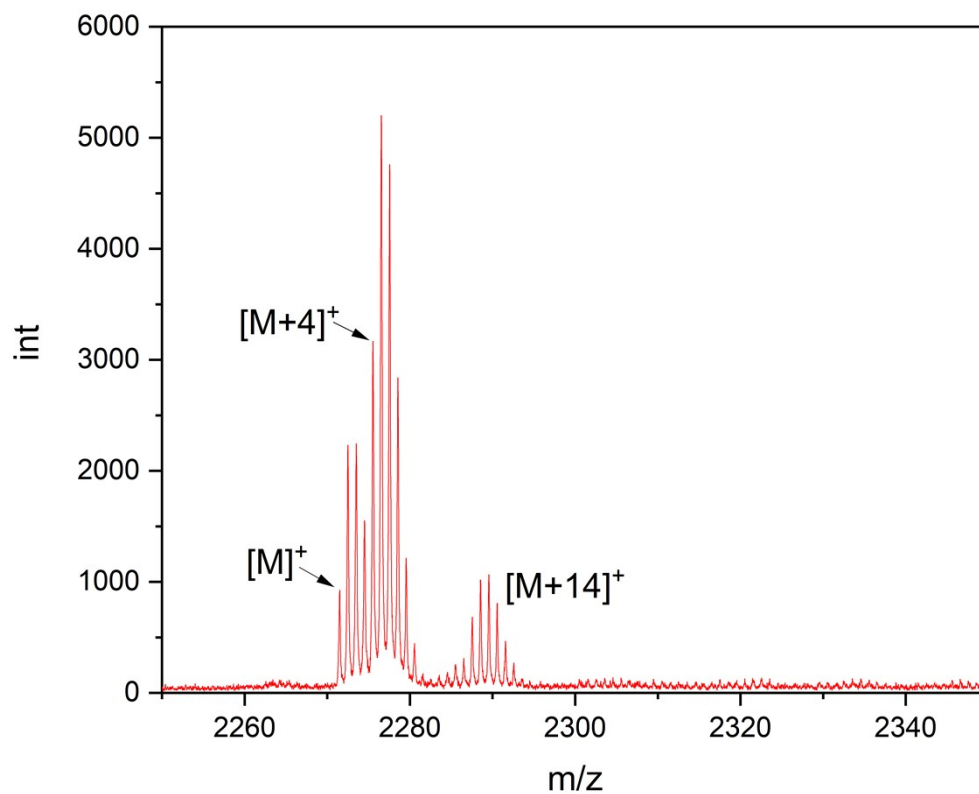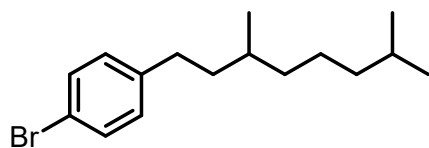

Figure S1. MALDI-TOF after Scholl reaction of **11** with FeCl$_3$. Conditions: 4 eq. FeCl$_3$/H, DCM/MeNO$_2$, -40 °C to rt, 3 d.

1.2.13 1-bromo-4-(3,7-dimethyloctyl)benzene (II)

II

A flame dried 10 mL Schlenk tube was charged with Mg turnings (309 mg, 12.7 mmol) and evacuated and flushed with argon three times. Dry THF (1 mL) was added and a splinter of iodine (approx. 20 mg) was added. The mixture was allowed to stir for 5 minutes. To the slightly red mixture, 1-bromo-3,7-dimethyloctane (469 mg, 2.12 mmol) was added dropwise. The mixture was brought to reflux and stirred overnight. Another flame dried 10 mL Schlenk tube was prepared by charging it with $ZnBr_2$ (478 mg, 2.12 mmol) and evacuating and flushing with argon three times. 1 mL dry THF was added. At 0°C, the Grignard solution was cannulated into the tube containing the zinc-bromide. After 45 minutes of stirring under cooling, 1-iodo-4-bromobenzene (500 mg, 1.77 mmol) and Pd(dppf)Cl_2 (26 mg, 35 µmol) were added. The mixture was brought to reflux and stirred overnight. After cooling to room temperature, the reaction was quenched by adding 2 mL of 1 M aq. HCl-solution. Water and dichloromethane were added and the aqueous layer was extracted three times with dichloromethane. The combined organic layers were dried by $MgSO_4$ and the crude product was filtrated over silica with dichloromethane as an eluent. Final purification was achieved by gel permeation chromatography (recycling-GPC) in chloroform. The product presented itself as a colorless liquid in 65% yield (340 mg, 1.14 mmol).

^{1}H NMR (500 MHz, CDCl$_3$) δ 7.38 (d, J = 8.3 Hz, 2H), 7.05 (d, J = 8.3 Hz, 2H), 2.63 – 2.47 (m, 2H), 1.62 – 1.49 (m, 2H), 1.46 – 1.37 (m, 2H), 1.33 – 1.22 (m, 3H), 1.17 – 1.10 (m, 3H), 0.92 (d, J = 6.4 Hz, 3H), 0.87 (d, J = 6.7 Hz, 6H).

^{13}C NMR (126 MHz, CDCl$_3$) δ 142.09, 131.26, 130.10, 119.18, 39.28, 38.78, 37.09, 32.89, 32.38, 27.94, 24.66, 22.69, 22.60, 19.55.

HR-MS (APCI): calc. m/Z =296.11396, exp. m/Z = 296.11429, error = +1.10 ppm.

1.2.14 Alkylchain equipped building block 12


12
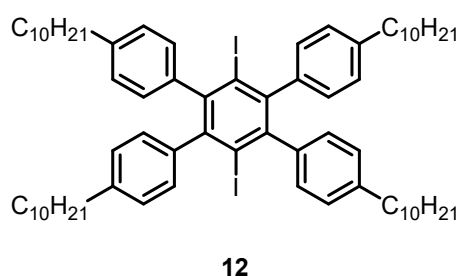
To a flame dried 25 mL Schlenk flask, Mg turnings (1.27 g, 52.2 mmol) were added. After evacuating and flushing with argon three times, dry THF (8.5 mL) was added. The reaction was allowed to stir with a crystal of iodine (approx. 20 mg) for 5 minutes at room temperature. Subsequently, 1-bromo-4-(3,7-dimethyloctyl)benzene (4.31 g, 14.5 mmol) was added and the mixture was brought to reflux and stirred overnight. A flame dried 100 mL Schlenk flask was charged with hexabromobenzene (800 mg, 1.5 mmol) and dry THF (7.5 mL) was added after evacuating and flushing the flask with argon three times. To avoid the formation of a slurry, the Grignard solution was cannulated to the 100 mL Schlenk flask while still hot. The mixture was stirred at room temperature overnight. The flask was then cooled via an ice bath and iodine (3.68g, 14.5 mmol) was added. After 30 minutes, the ice bath was removed and the mixture was allowed to stir for 90 more minutes at room temperature. The reaction was quenched by 30 mL of saturated aq. $Na_2S_2O_3$-solution. Dichloromethane and water were added and the aqueous layer was extracted three times with dichloromethane. The combined organic layers were dried by $MgSO_4$ and the crude product was filtrated over silica with dichloromethane as an eluent. Final purification was achieved by recycling-GPC using chloroform as an eluent. The product was isolated as a colorless solid in 61% yield (1.06 g, 0.9 mmol).

^{1}H NMR (500 MHz, CDCl$_3$) δ 7.02 – 6.83 (m, 16H), 2.58 – 2.40 (m, 8H), 1.56 – 1.49 (m, 8H), 1.37 – 1.23 (m, 20H), 1.17 – 1.05 (m, 12H), 0.93 – 0.79 (m, 36H).

^{13}C NMR (126 MHz, CDCl$_3$) δ 146.43, 143.03, 141.52, 129.69, 127.23, 108.46, 39.32, 38.59, 37.10, 33.13, 32.36, 27.95, 24.70, 22.72, 22.64, 19.65.

HR-MS (APCI): calc. m/Z =1194.59144, exp. m/Z = 1194.59109, error = -0.29 ppm.

P1
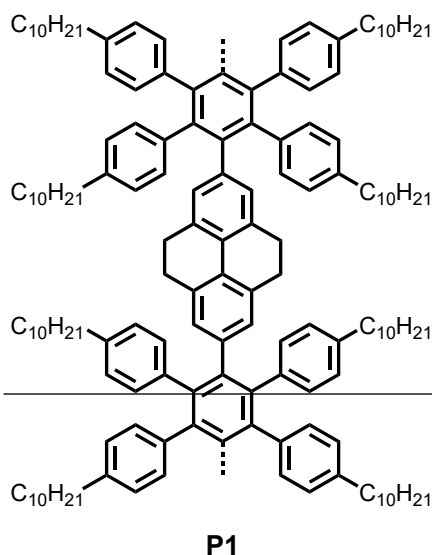
1.2.15 Polymer P1

A 50 mL Schlenk tube was charged with compound **11** (569 mg, 476 µmol), compound **4** (218 mg, 476 µmol) and potassium carbonate (3.29 g, 23.8 mmol).

After evacuating and flushing with argon three times, toluene (20 mL) and water (5 mL) were added. The tip of a cannula was dipped in Aliquat 336 and subsequently used to flush the mixture with argon for 20 minutes. Afterwards, $Pd(PPh_3)_4$ (28 mg, 24 μmol) was added, the flask was sealed and brought to reflux for 48 hours. After cooling to room temperature, the mixture was poured into a mixture of methanol (200 mL) and conc. aq. HCl-solution (20 mL). After stirring for 5 minutes at room temperature, the mixture was filtered. The residue was dissolved in chloroform and filtered once more to remove remaining solids. After evaporation of the solvent, **P1** was obtained as a slightly orange solid in 92% yield (503 mg).

^{1}H NMR (500 MHz, CDCl$_3$) δ 6.73 – 6.56 (m, 16H), 6.30 (s, 4H), 2.43 – 2.25 (m, 8H), 2.15 (s, 8H), 1.60 – 0.99 (m, 40H), 0.86 (d, J = 6.5 Hz, 24H), 0.80 (d, J = 6.0 Hz, 12H).

^{13}C NMR (126 MHz, CDCl$_3$) δ 140.27, 139.28, 138.47, 132.88, 131.47, 129.85, 129.38, 127.39, 127.22, 126.32, 39.38, 39.31, 39.04, 37.11, 33.01, 32.30, 27.94, 24.66, 22.72, 22.64, 19.59.

For mass spectra see Figure S32.

1.2.16 Graphenenanoribbon PyGNR
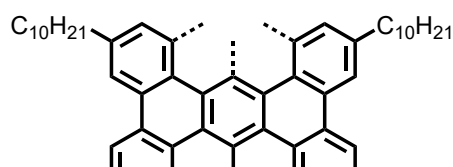
A flame dried 25 mL Schlenk flask was charged with polymer **P1** (10 mg) and evacuated/flushed with
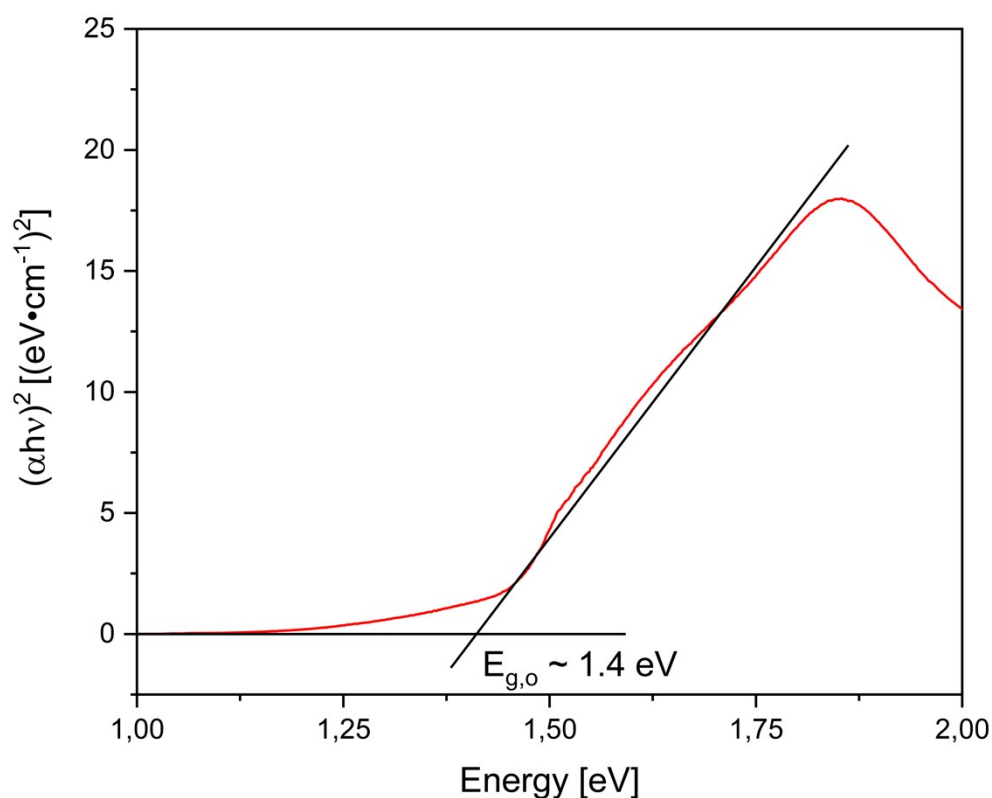
argon three times. 10 mL of dry and degassed dichloromethane were added, followed by a suspension of $FeCl_3$ (158 mg, 7 eq./H) in dry and degassed $MeNO_2$ (1 mL). The black mixture was allowed to stir at room temperature for a full week. The reaction mixture was then diluted with MeOH and filtrated. The residue was washed three times with small portions of MeOH and dried under reduced pressure. **PyGNR** was obtained as a black powder in 90% yield (9 mg).

Figure S2. Tauc-plot for the UV-Vis spectra of **PyGNR**.

2 NMR Spectra

2.1 2,7-bis(4,4,5,5-tetramethyl-1,3,2-dioxaborolan-2-yl)-4,5,9,10-
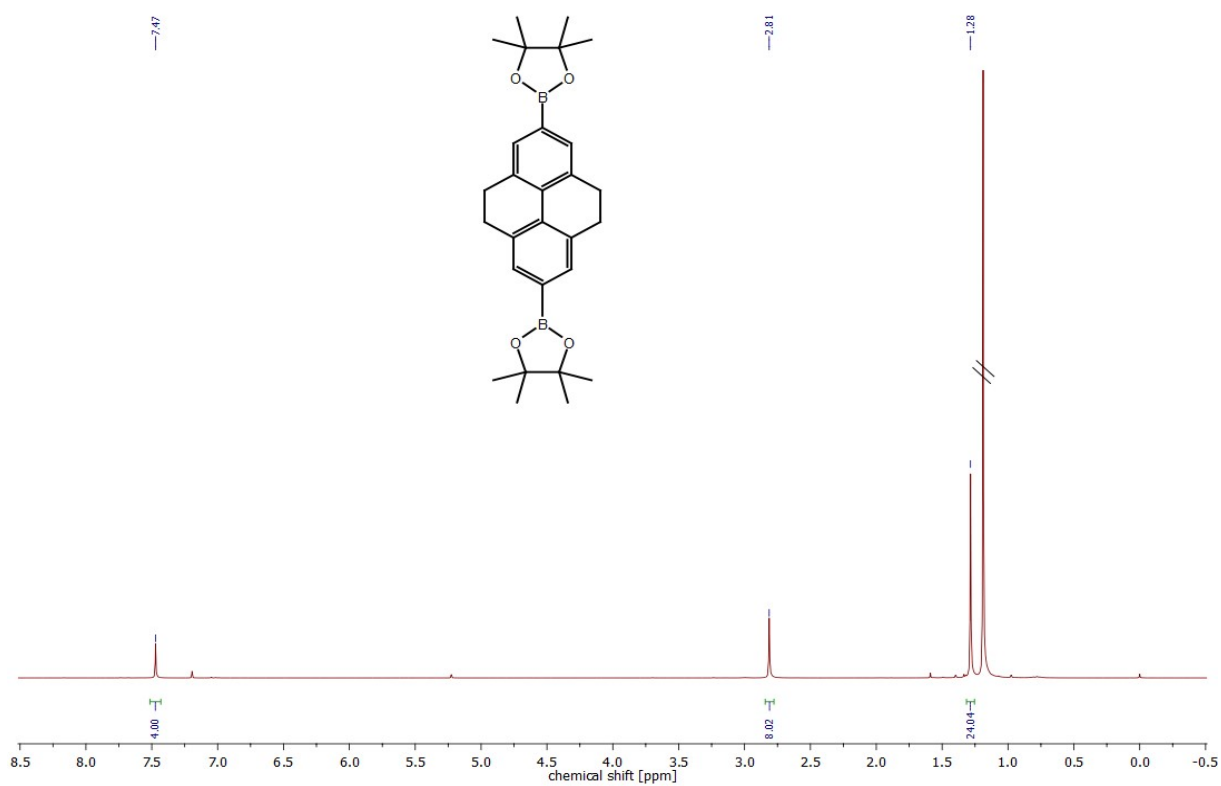
tetrahydropyrene (4)
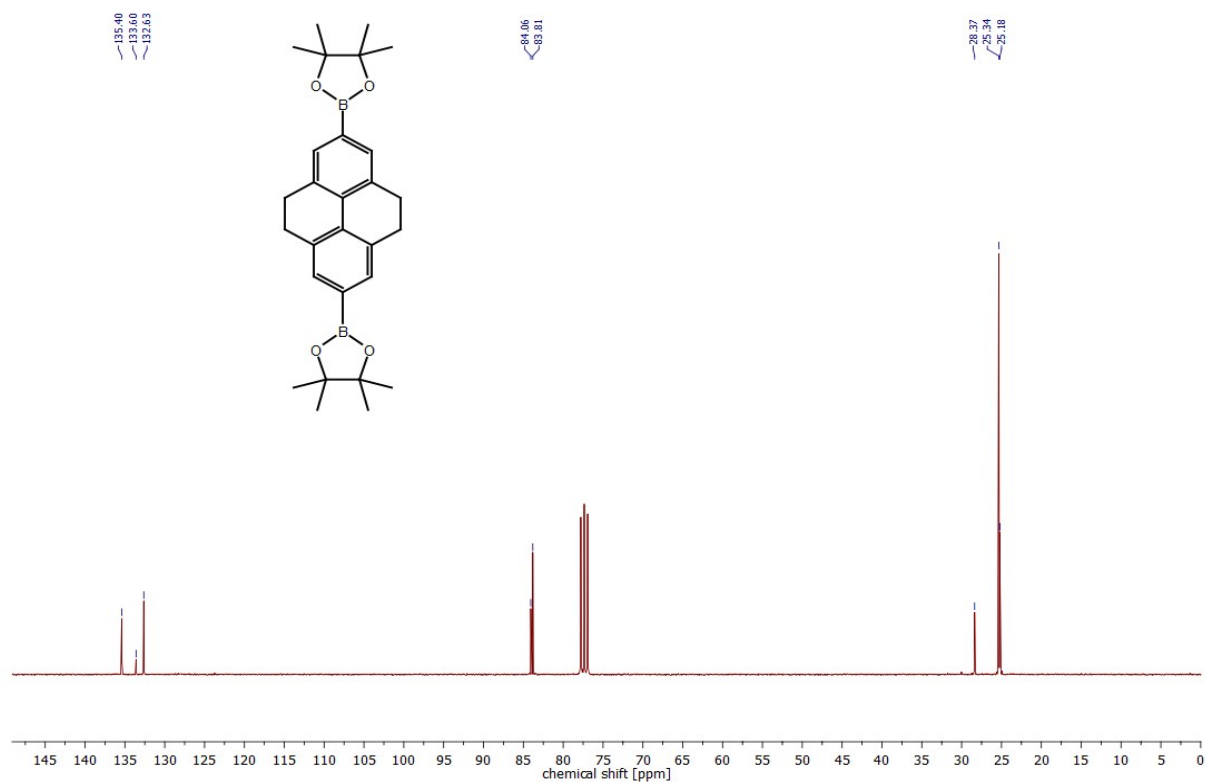
Figure S3. ^{1}H-NMR spectra of **4** (300 MHz, CD$_2$Cl$_2$).

Figure S4. ^{13}C-NMR spectra of **4** (75 MHz, CDCl$_3$).

2.2 4'-Bromo-2,4,6-trimethyl-1,1'-biphenyl (I)
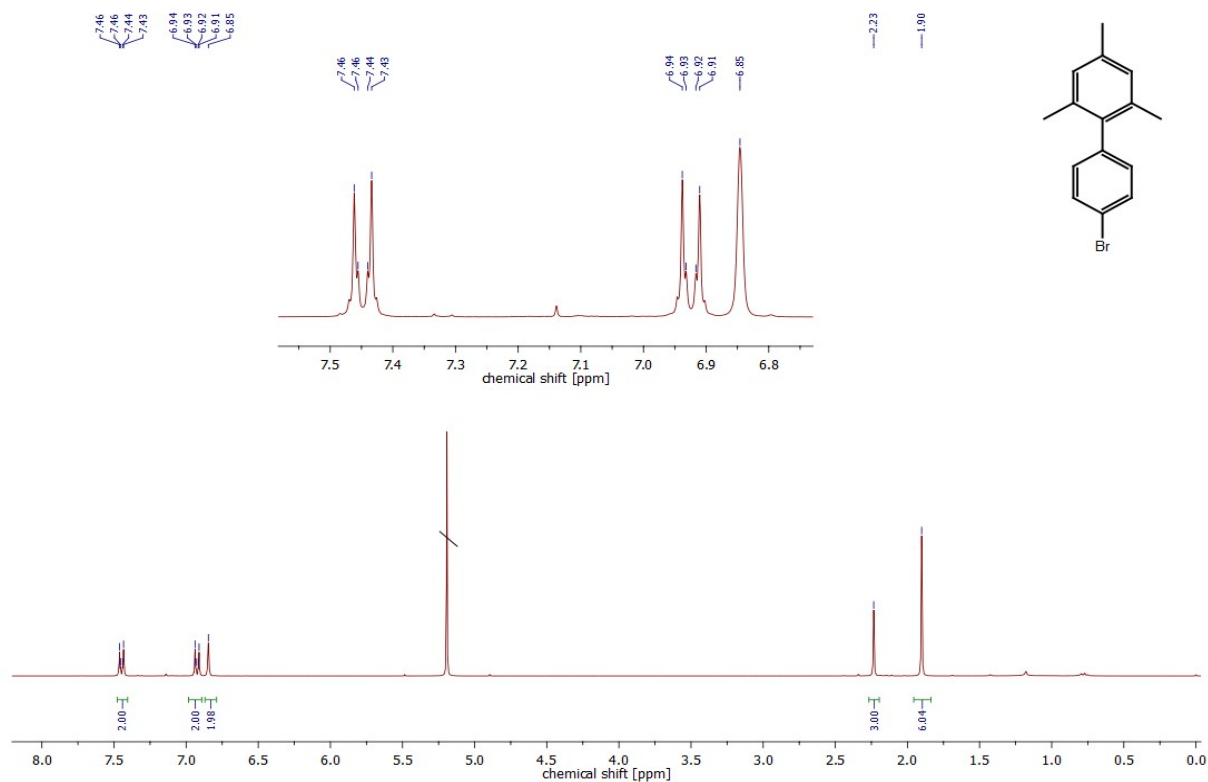
Figure S5. ^{1}H-NMR spectra of **I** (300 MHz, CDCl$_3$).
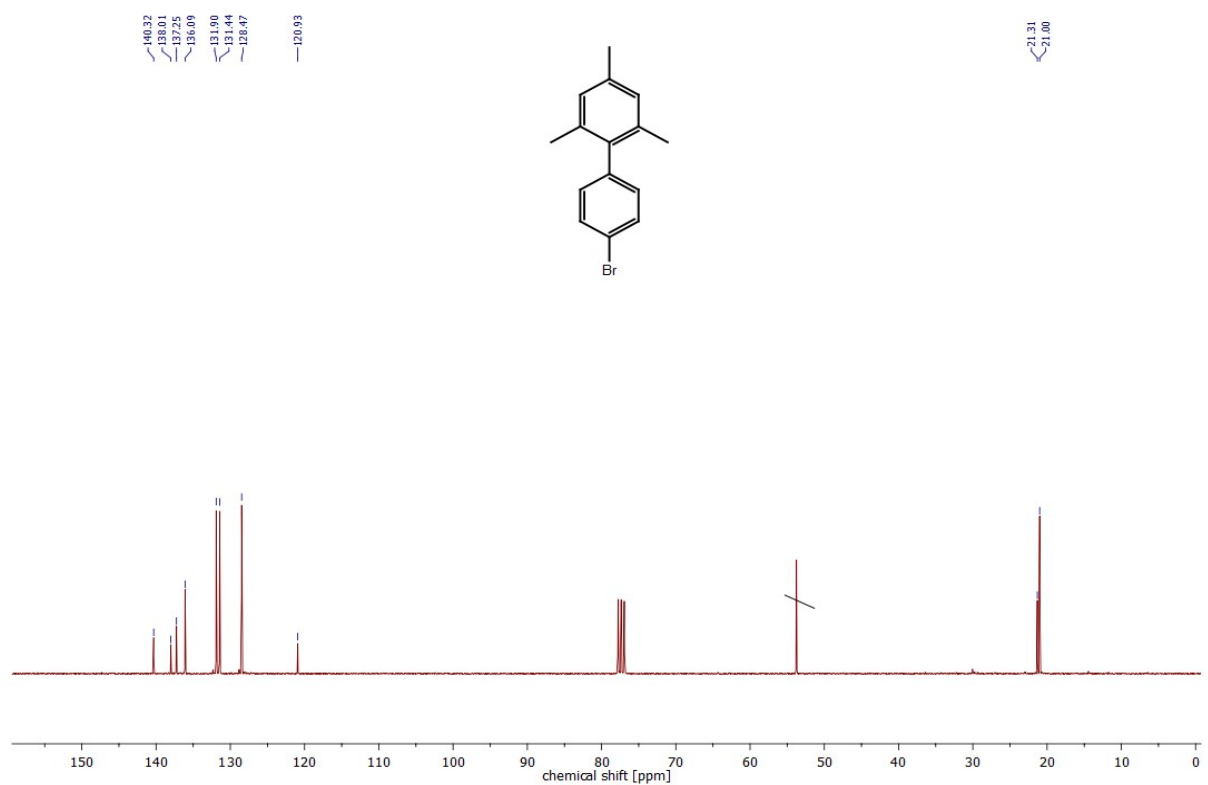
Figure S6. ^{13}C-NMR spectra of **I** (76 MHz, CDCl$_3$).

2.3   4,4,5,5-tetramethyl-2-(2',4',6'-trimethyl-[1,1'-biphenyl]-4-yl)-1,3,2-dioxaborolane (6)
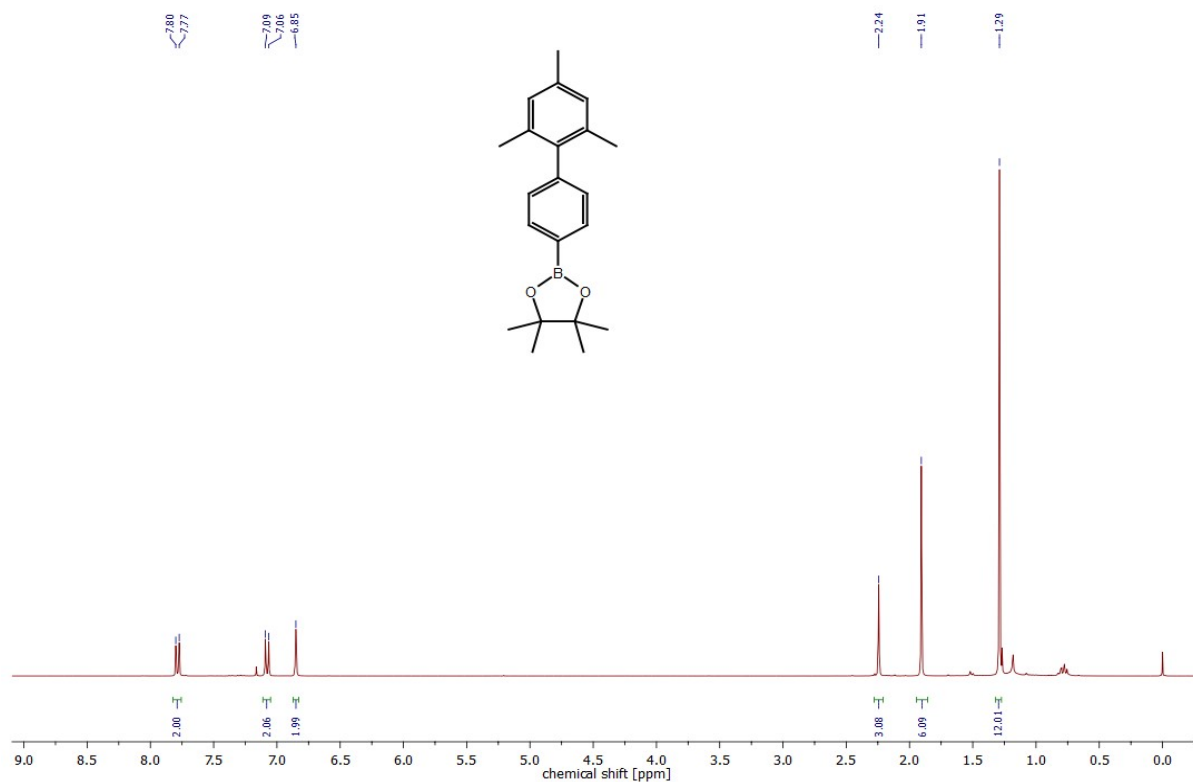
Figure S7. ^{1}H-NMR spectra of **6** (300 MHz, CDCl$_3$).
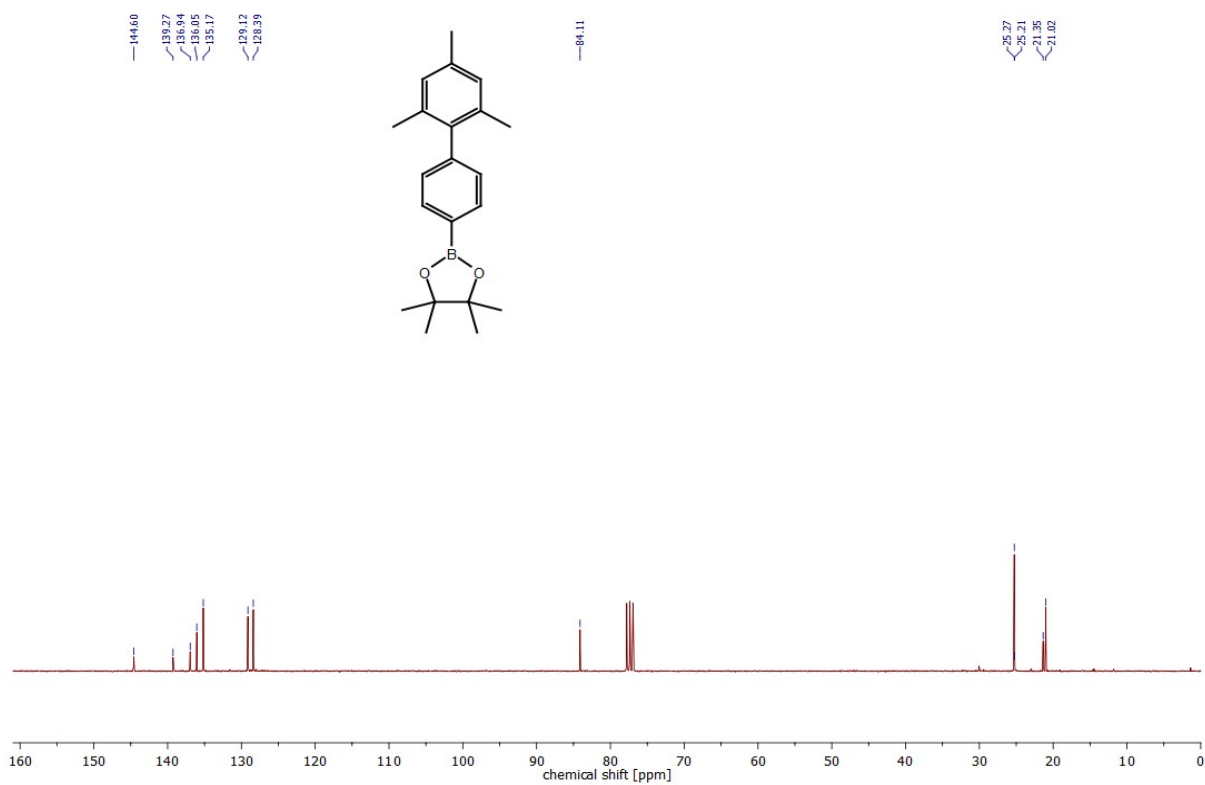
Figure S8. ^{13}C-NMR spectra of **6** (76 MHz, CDCl$_3$).

2.4   1,2,3-tribromo-5-nitrobenzene (5)
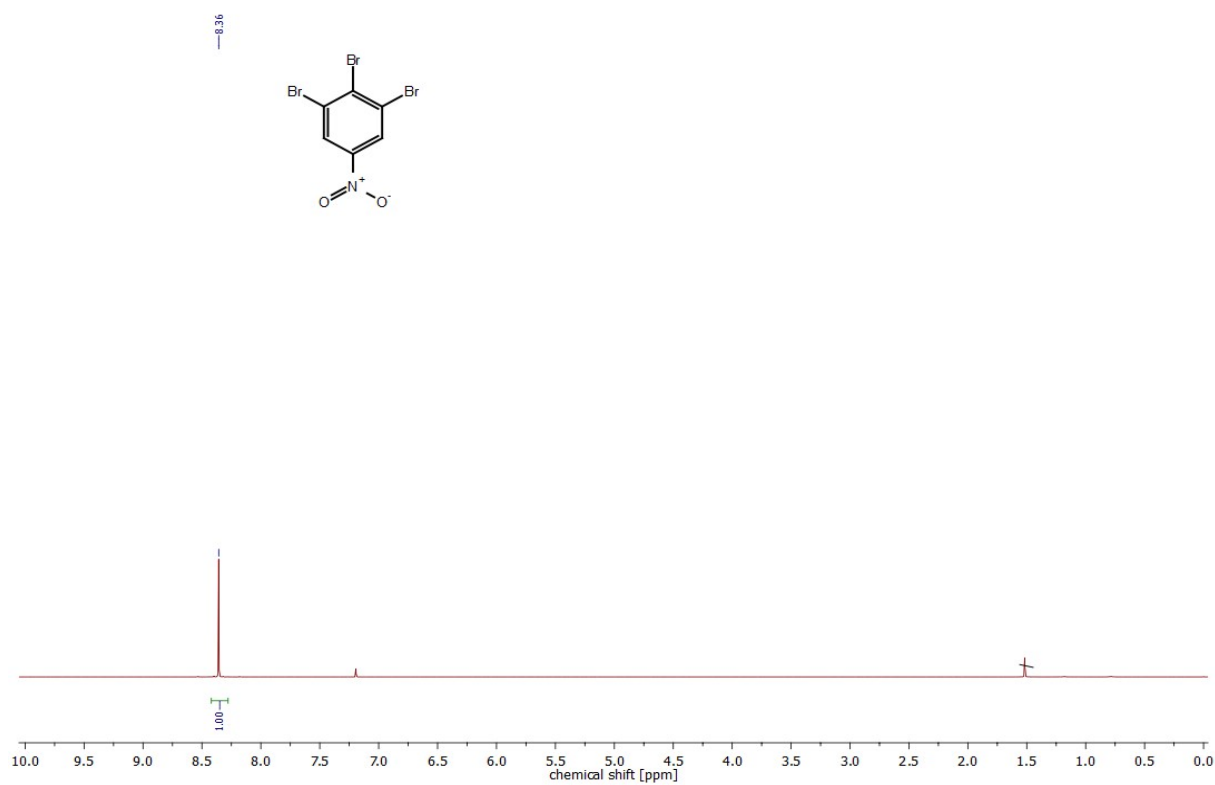
Figure S9. ^{1}H-NMR spectra of 1,2,3-tribromo-5-nitrobenzene (**5**, 500 MHz, CDCl$_3$).
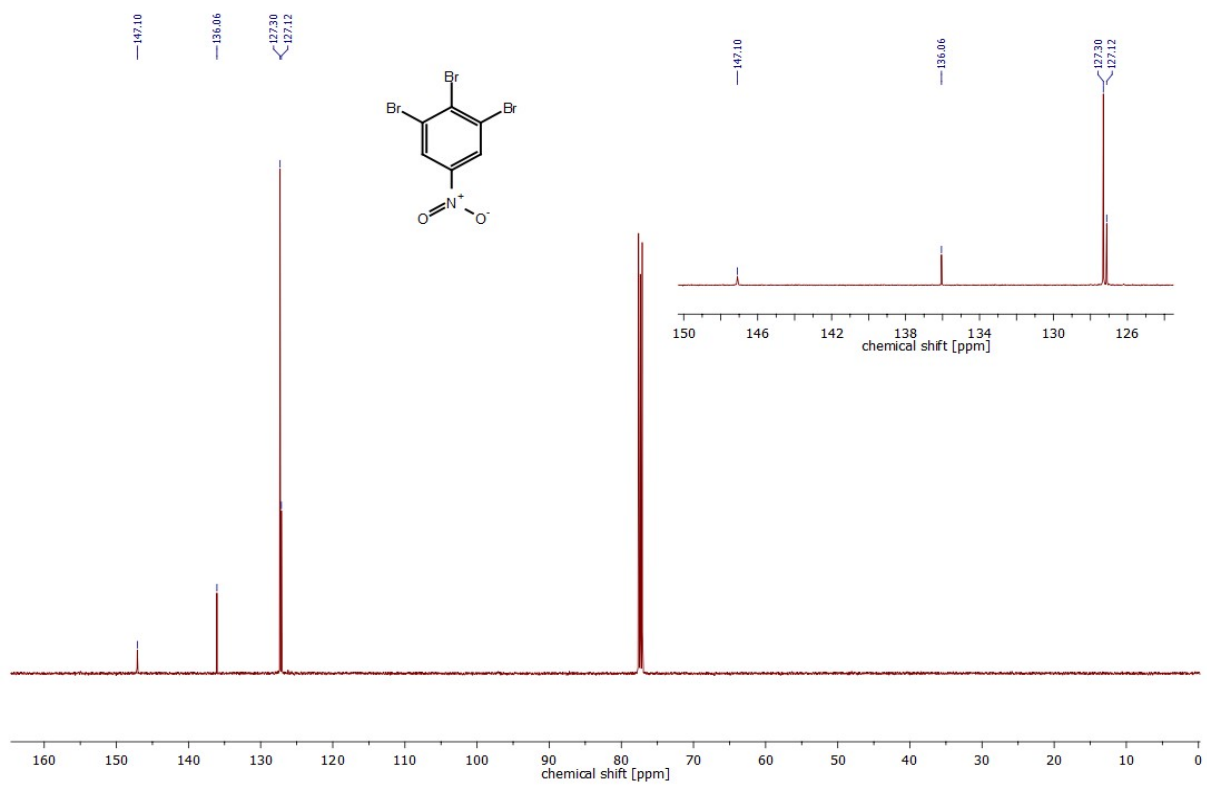
Figure S10. ^{13}C-NMR spectra of 1,2,3-tribromo-5-nitrobenzene (**5**, 126 MHz, CDCl$_3$).

2.5 Compound 7
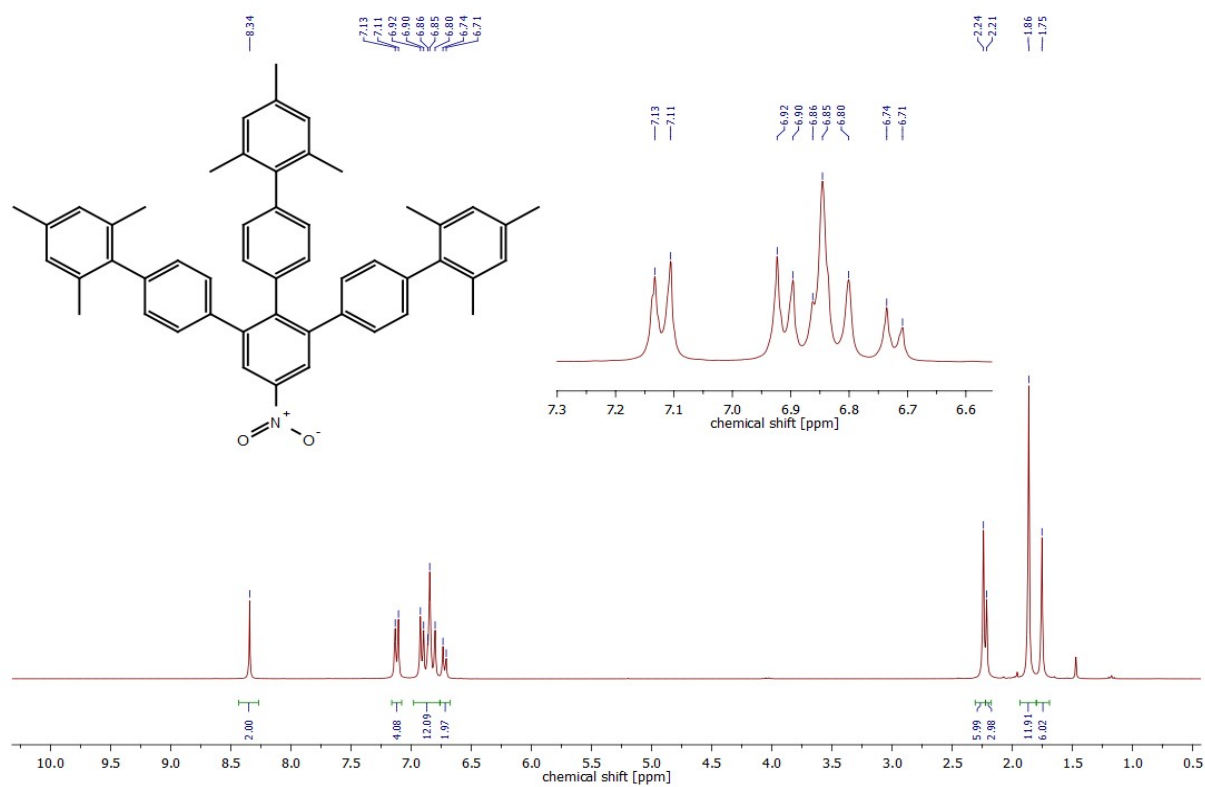
Figure S11. ^{1}H-NMR spectra of compound **7** (500 MHz, CDCl$_3$).
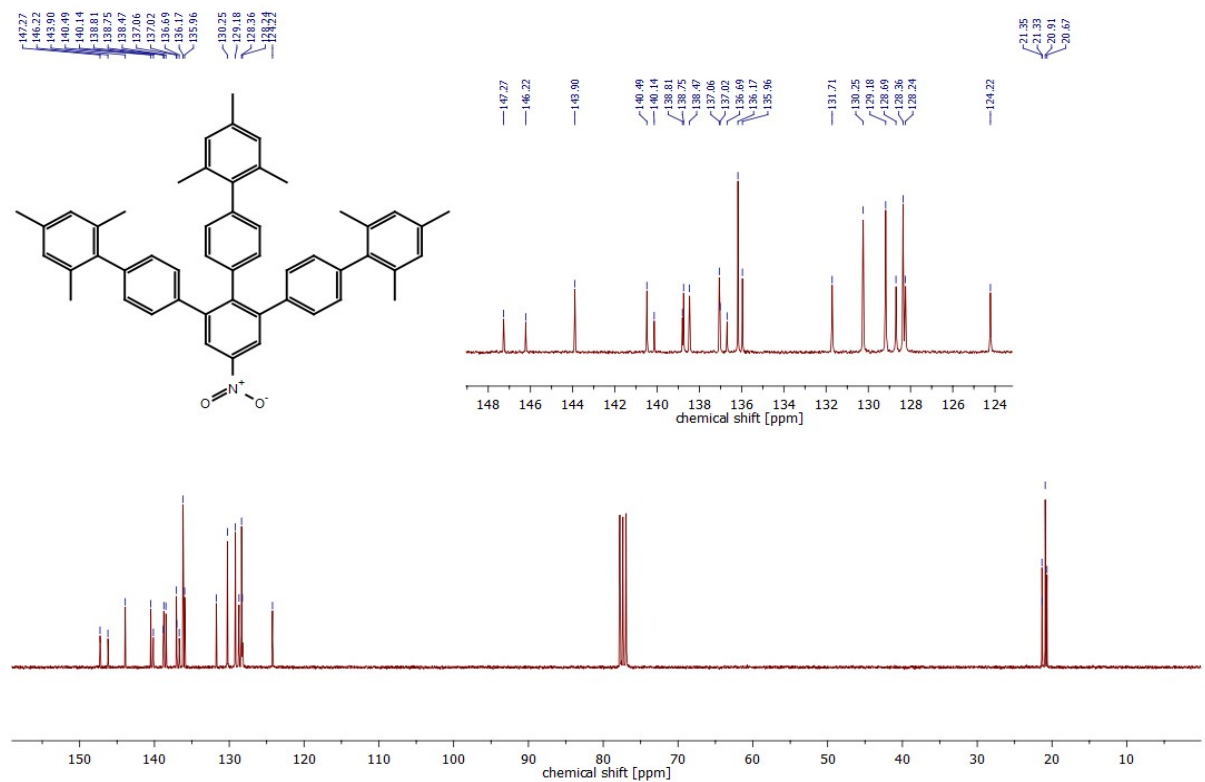
Figure S12. ^{13}C-NMR spectra of compound **7** (126 MHz, CDCl$_3$).

2.6   Compound 8
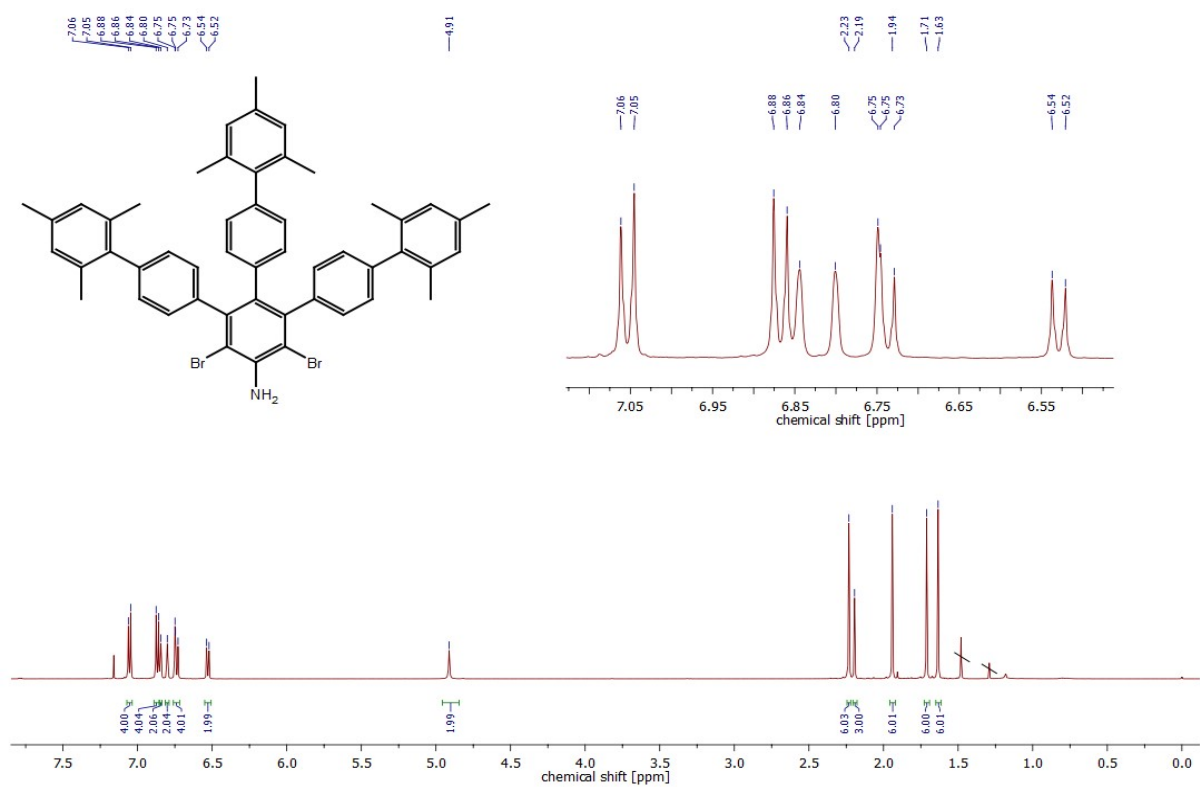
Figure S13. ^{1}H-NMR spectra of compound **8** (500 MHz, CDCl$_3$).
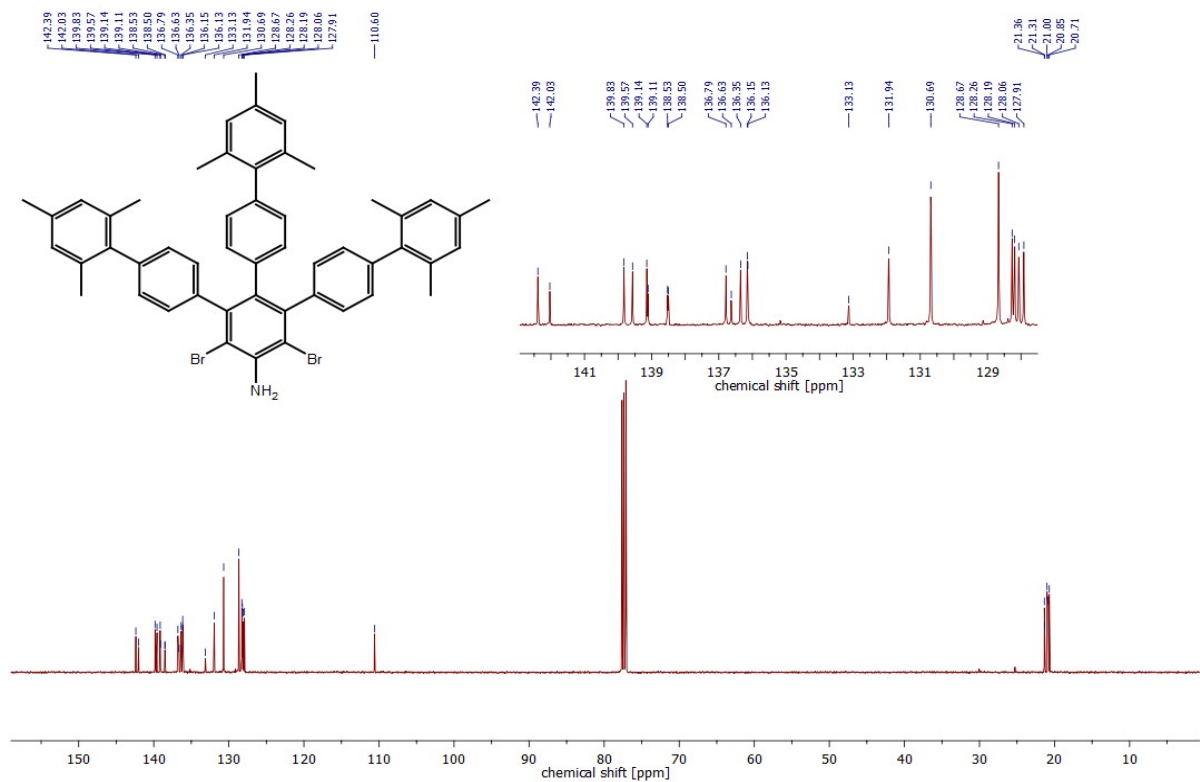
Figure S14. ^{13}C-NMR spectra of compound **8** (126 MHz, CDCl$_3$).

2.7 Compound 9

Figure S15. ^{1}H-NMR spectra of compound **9** (500 MHz, CD_2Cl_2).

Figure S16. ^{13}C-NMR spectra of compound **9** (126 MHz, $CDCl_3$).

2.8 Building Block 10
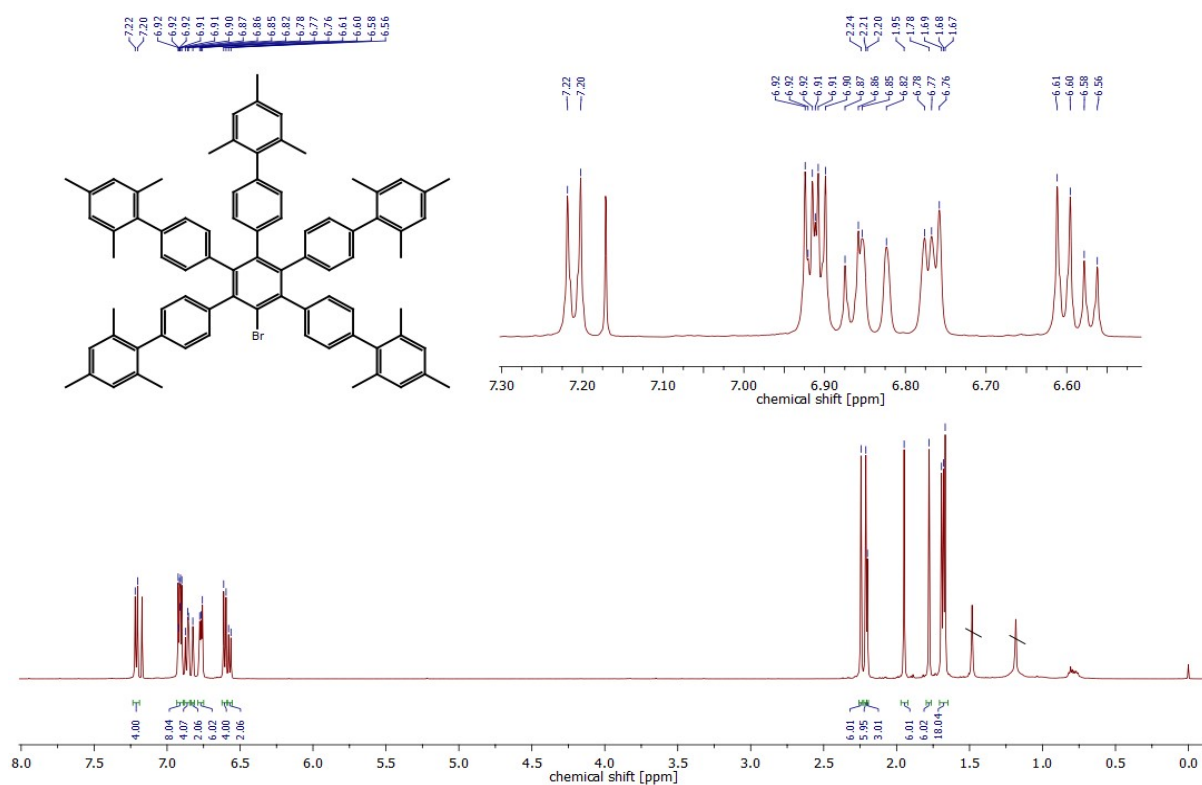
Figure S17. ¹H-NMR spectra of compound **10** (500 MHz, CDCl₃).
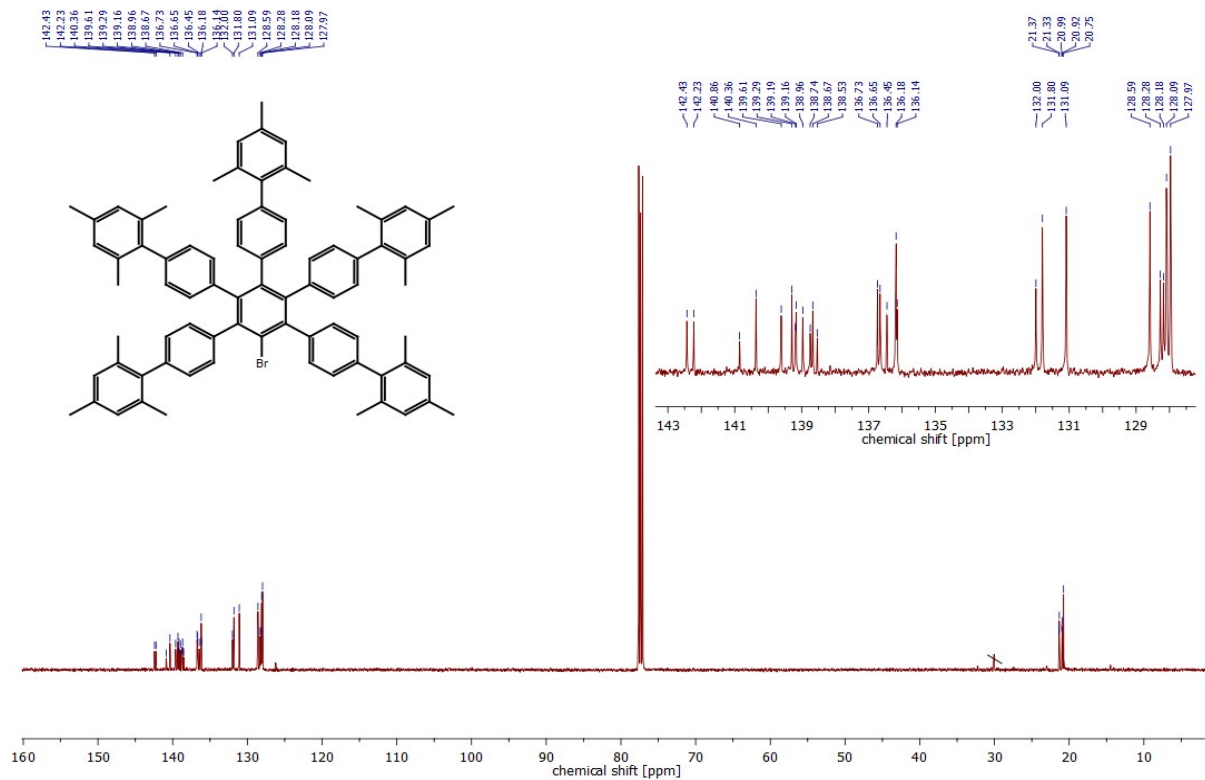
Figure S18. ¹³C-NMR spectra of compound **10** (126 MHz, CDCl₃).

2.9 Model compound precursor 11
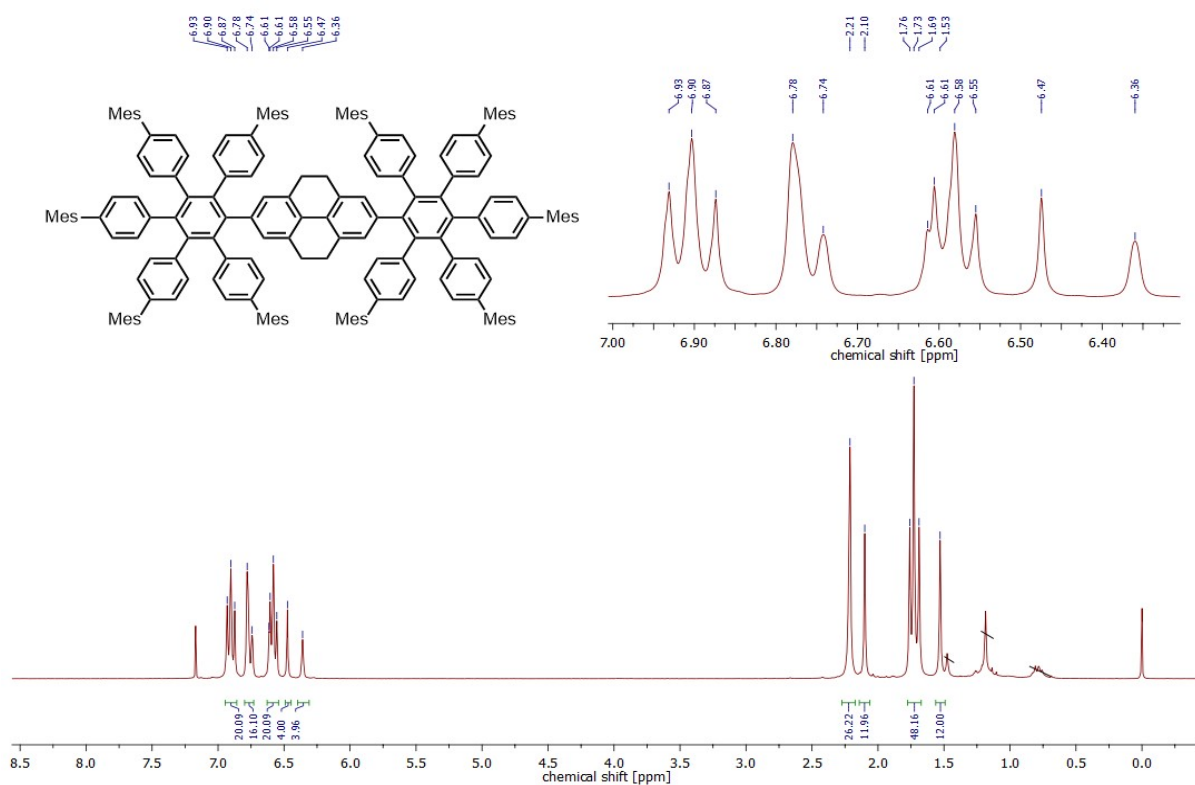
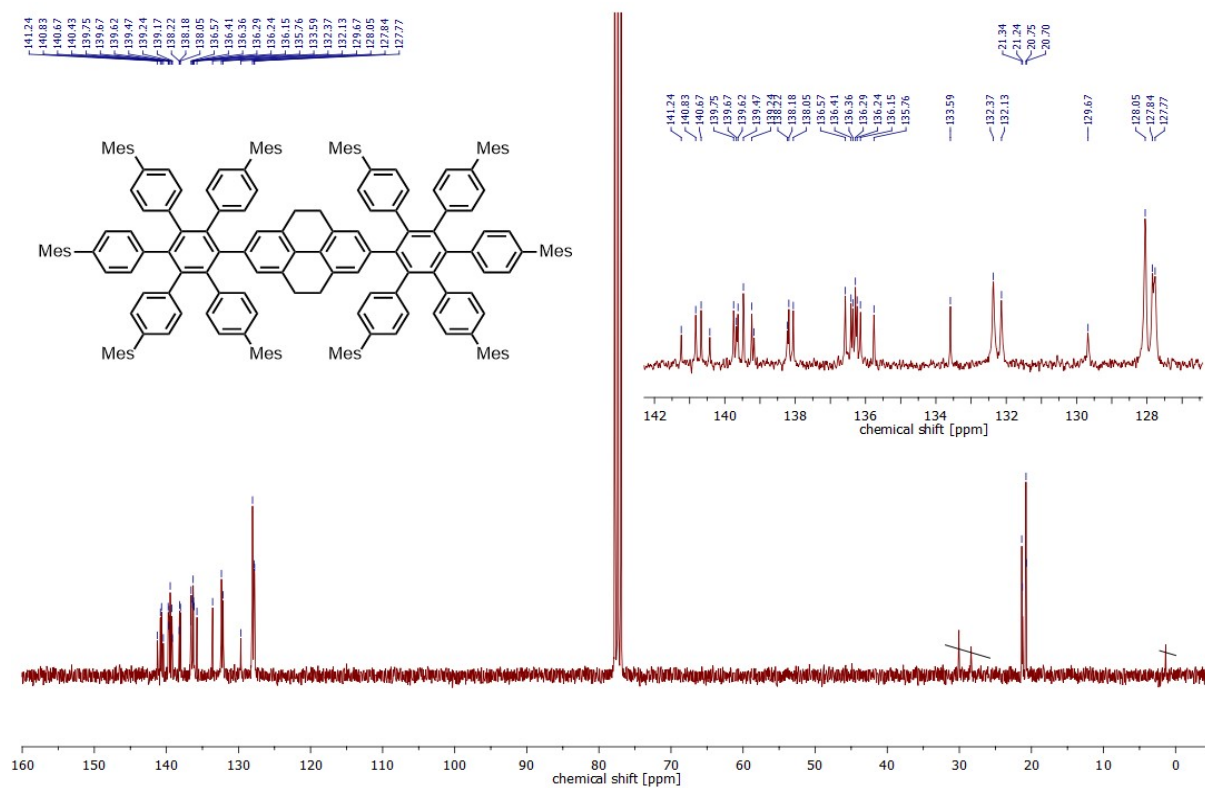**Figure S19.** ^{1}H-NMR spectra of compound **11** (300 MHz, CDCl$_3$).

Figure S20. ^{13}C-NMR spectra of compound **11** (76 MHz, CDCl$_3$).
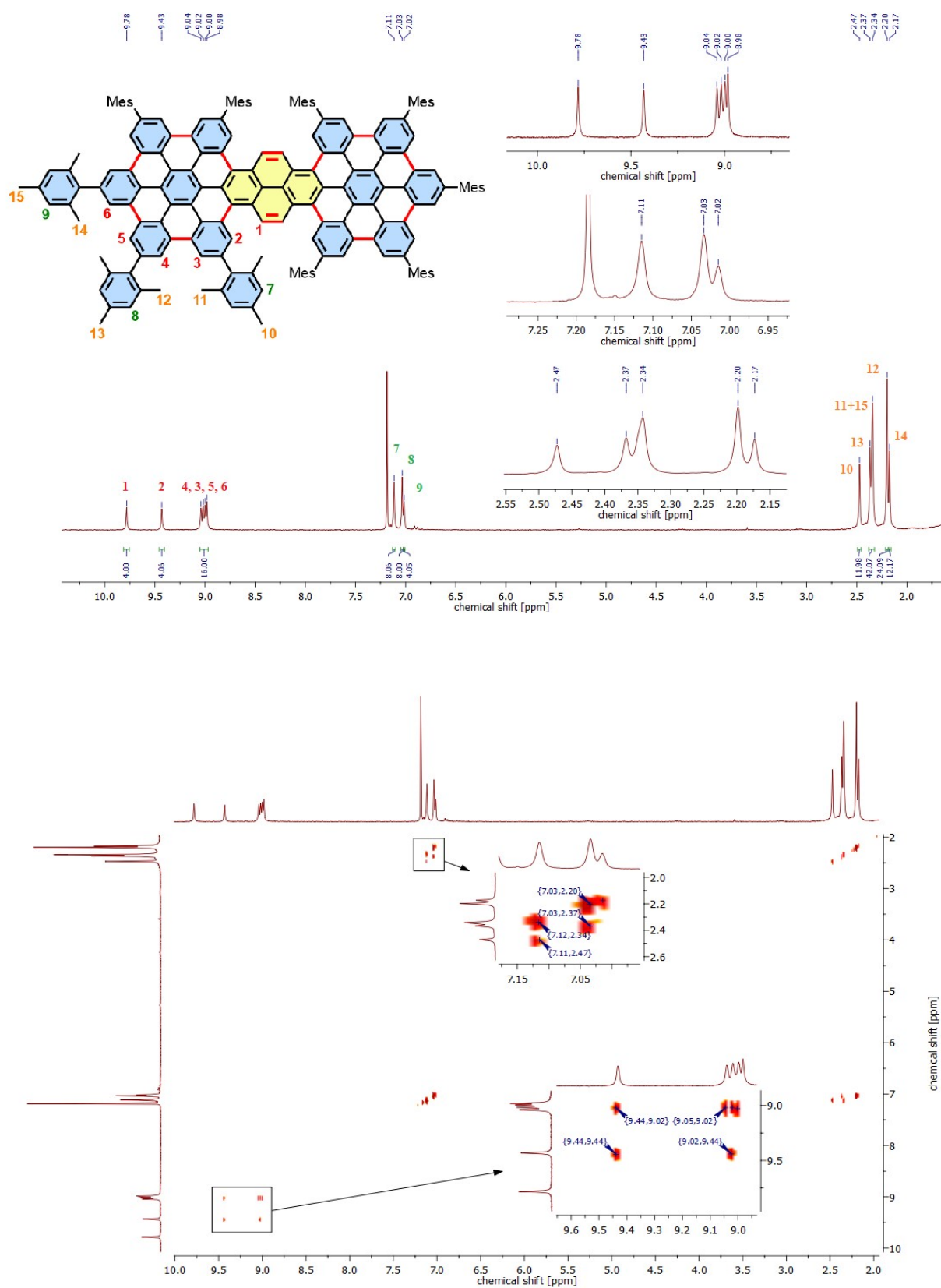
2.10 Model compound 1

Figure S21. ^{1}H-NMR spectra of compound **1** (300 MHz, CDCl$_3$).

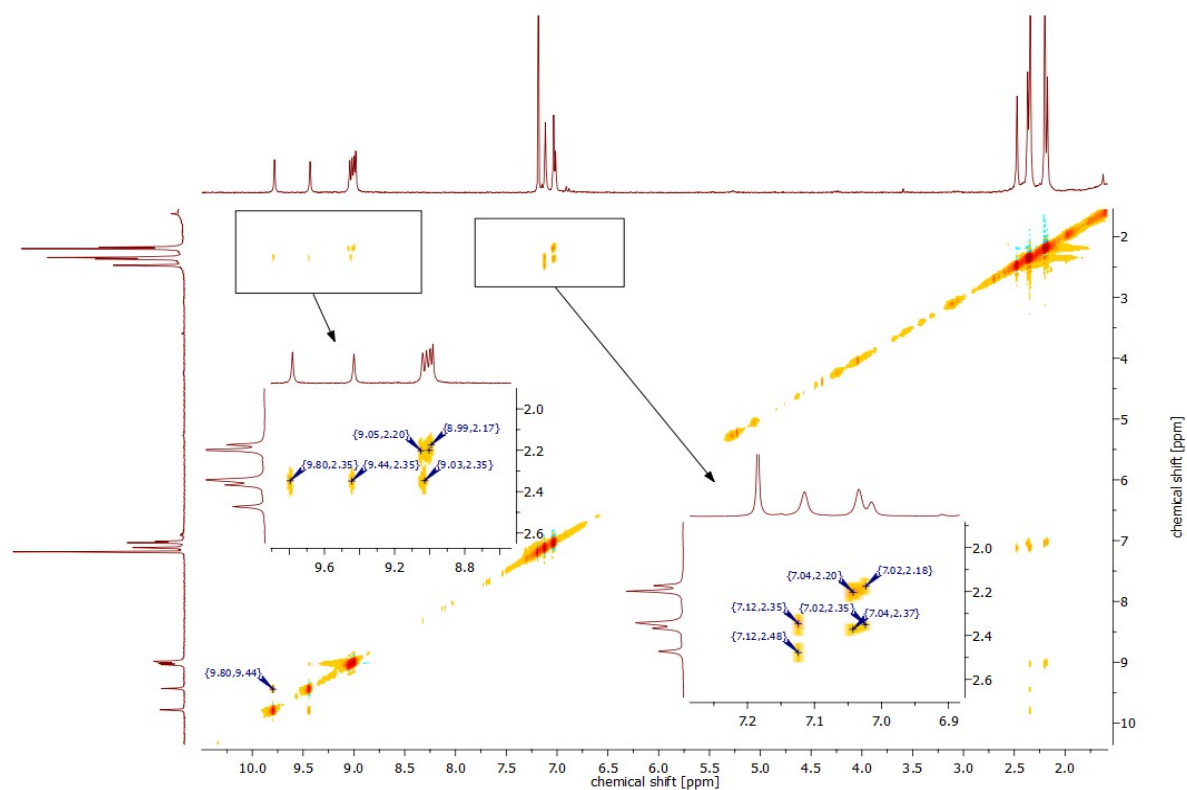**Figure S22.** COSY-spectra of compound **1** (300 MHz, CDCl$_3$).

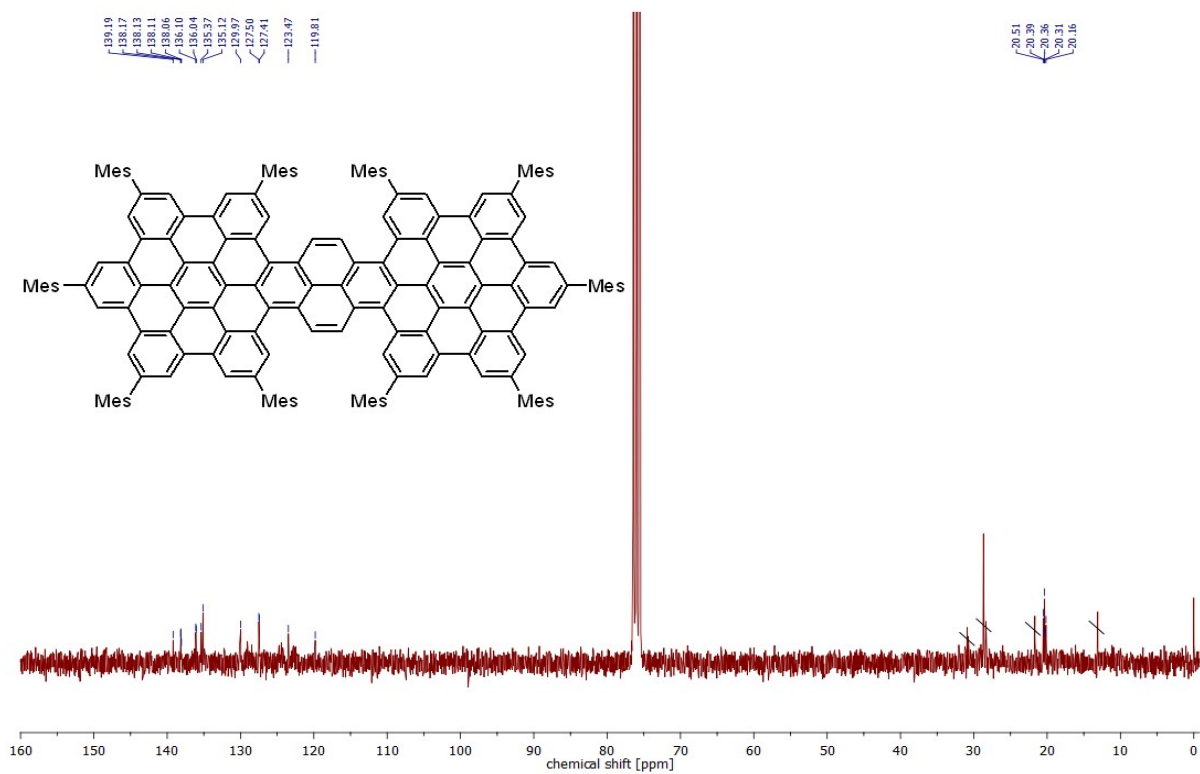**Figure S23.** NOESY-spectra of compound **1** (300 MHz, CDCl$_3$).

Figure S24. ^{13}C-NMR spectra of compound **1** (75 MHz, CDCl$_3$).
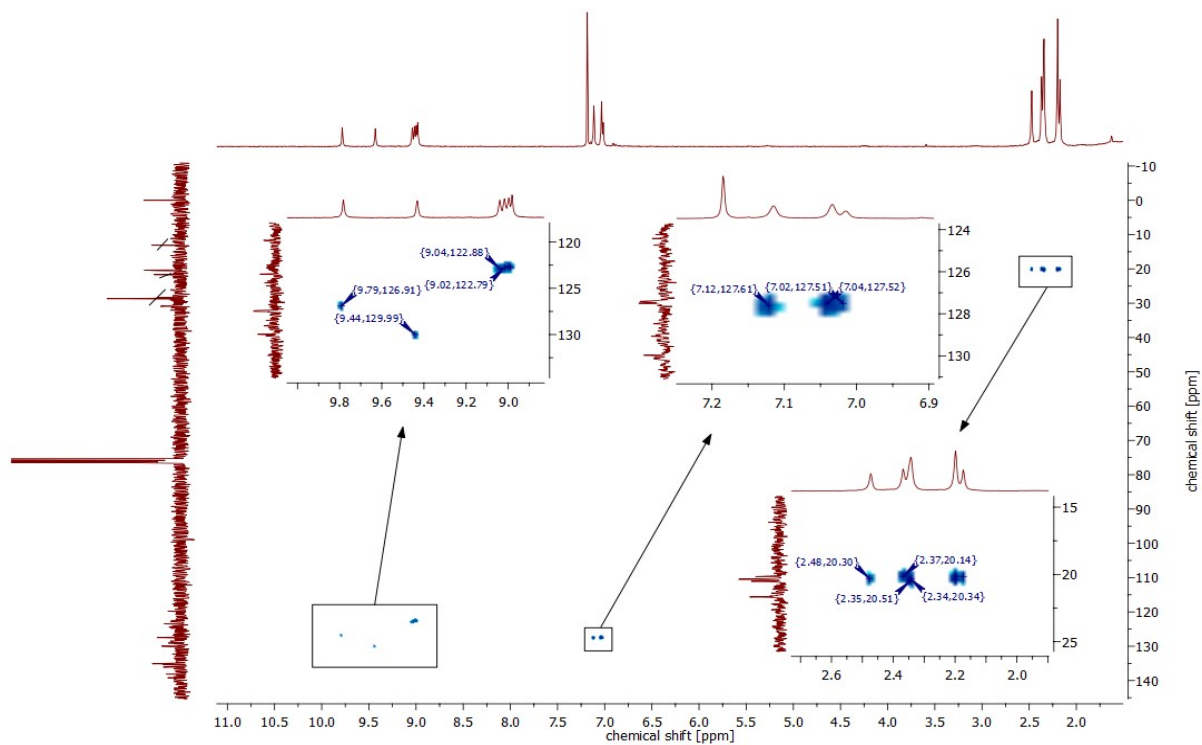
Figure S25. HSQC-Experiment of compound **1** (300/75 MHz, CDCl$_3$).

2.11 1-Bromo-4-(3,7-dimethyloctyl)benzene (II)

Figure S26. ^{1}H-NMR spectra of compound **II** (500 MHz, CDCl$_3$).

Figure S27. ^{13}C-NMR spectra of compound **II** (126 MHz, CDCl$_3$).

2.12 Alkyl chain equipped building block 12
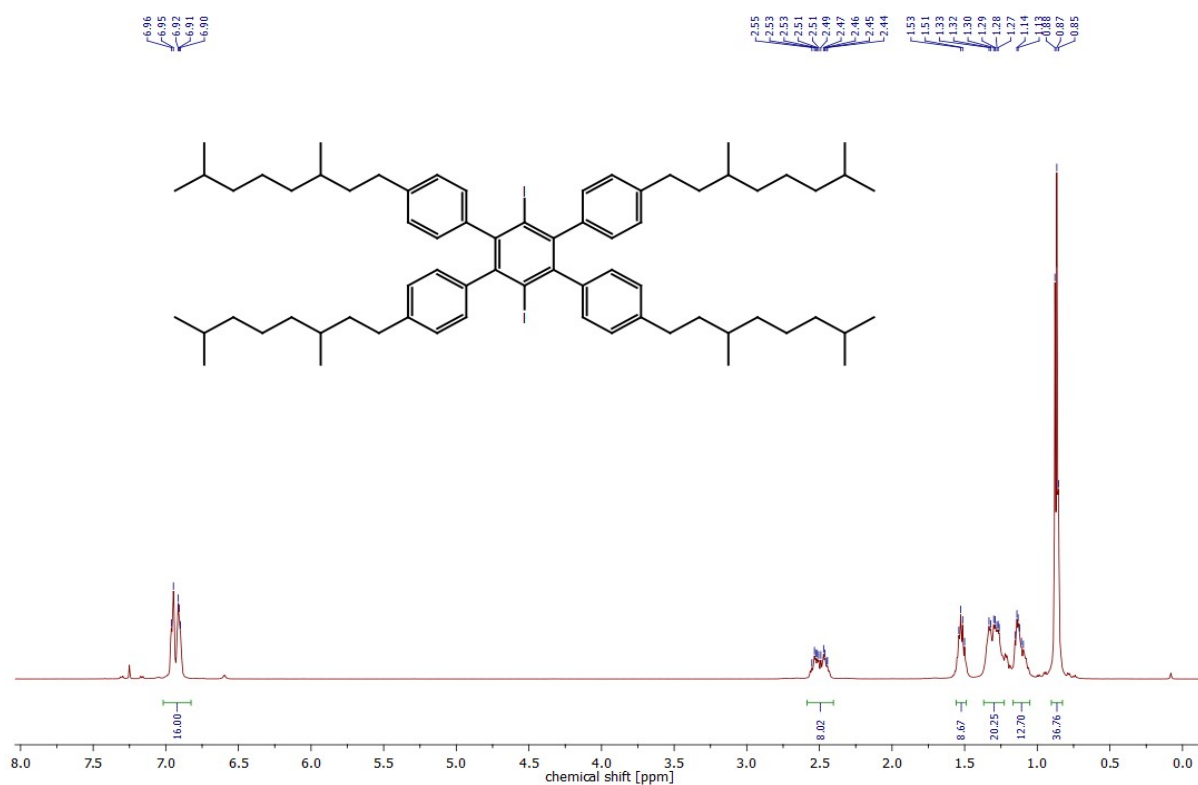
Figure S28. ^{1}H-NMR spectra of compound **12** (500 MHz, CDCl$_3$).
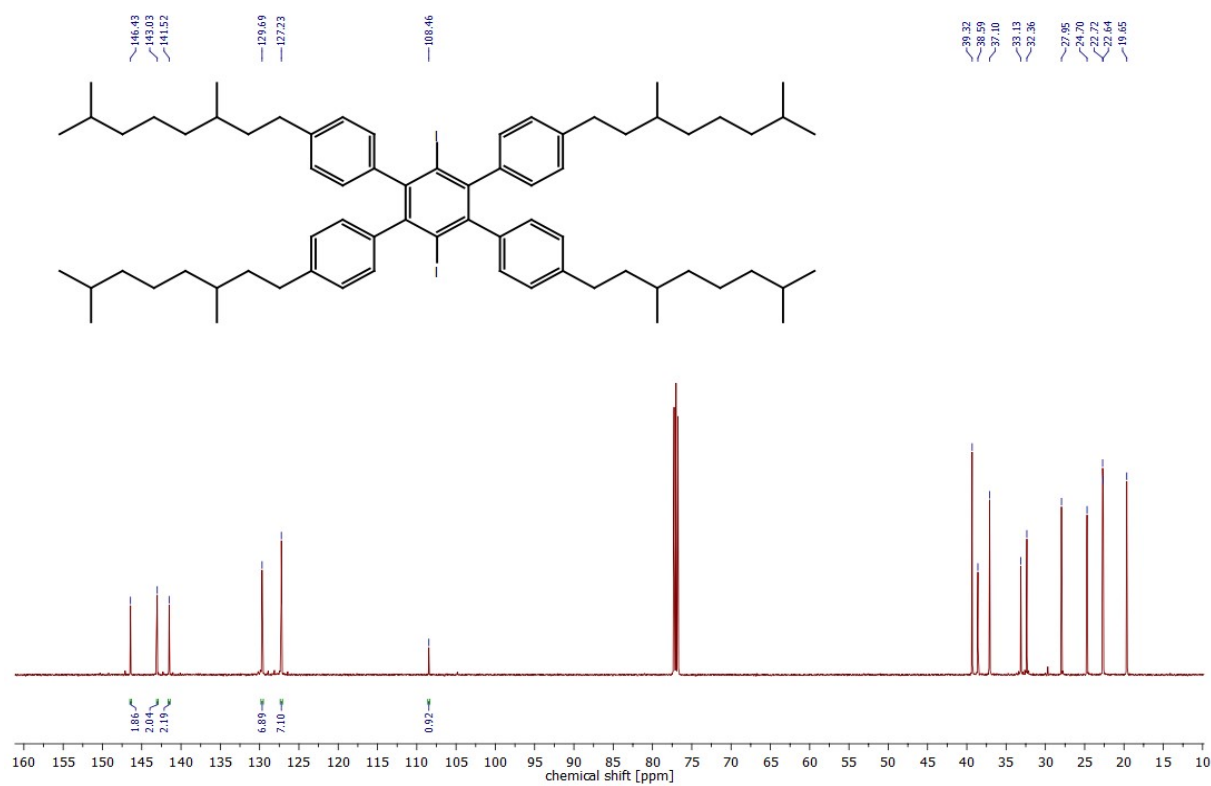
Figure S29. ^{13}C-NMR spectra of compound **12** (126 MHz, CDCl$_3$).

2.13 Polymer P1
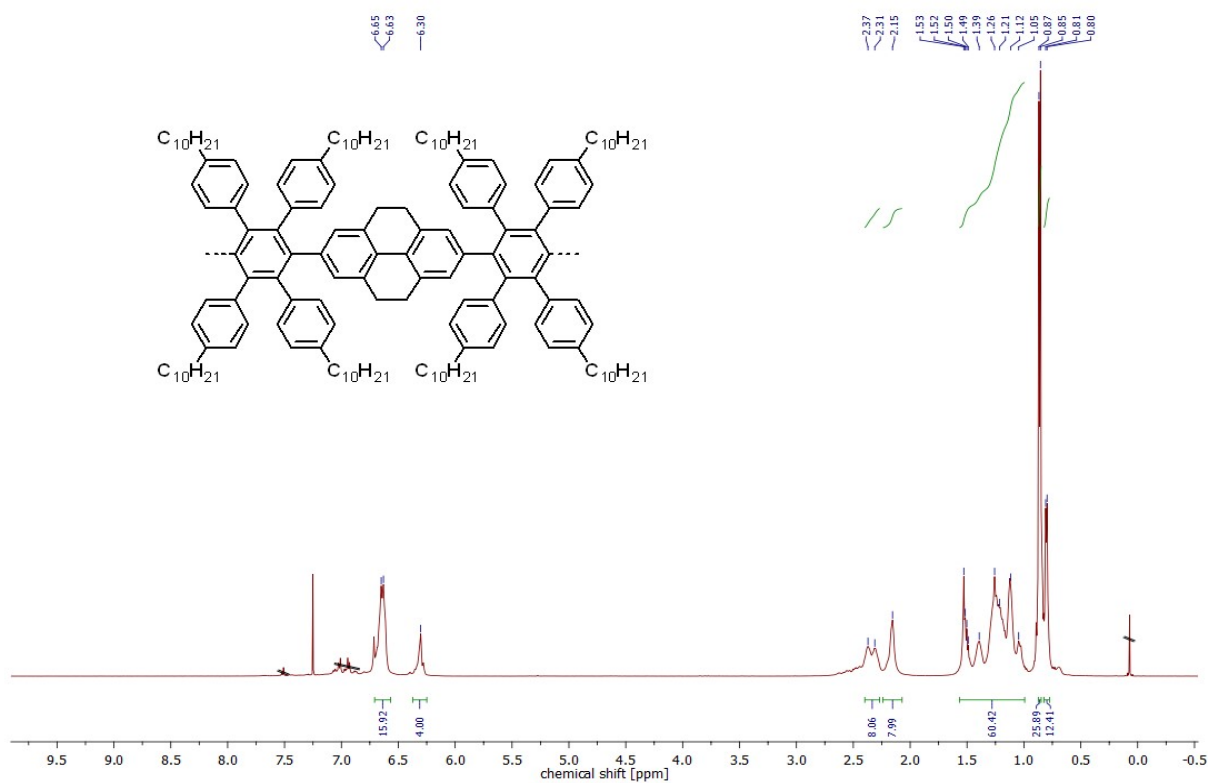
Figure S30. ^{1}H-NMR spectra of polymer **P1** (500 MHz, CDCl$_3$).
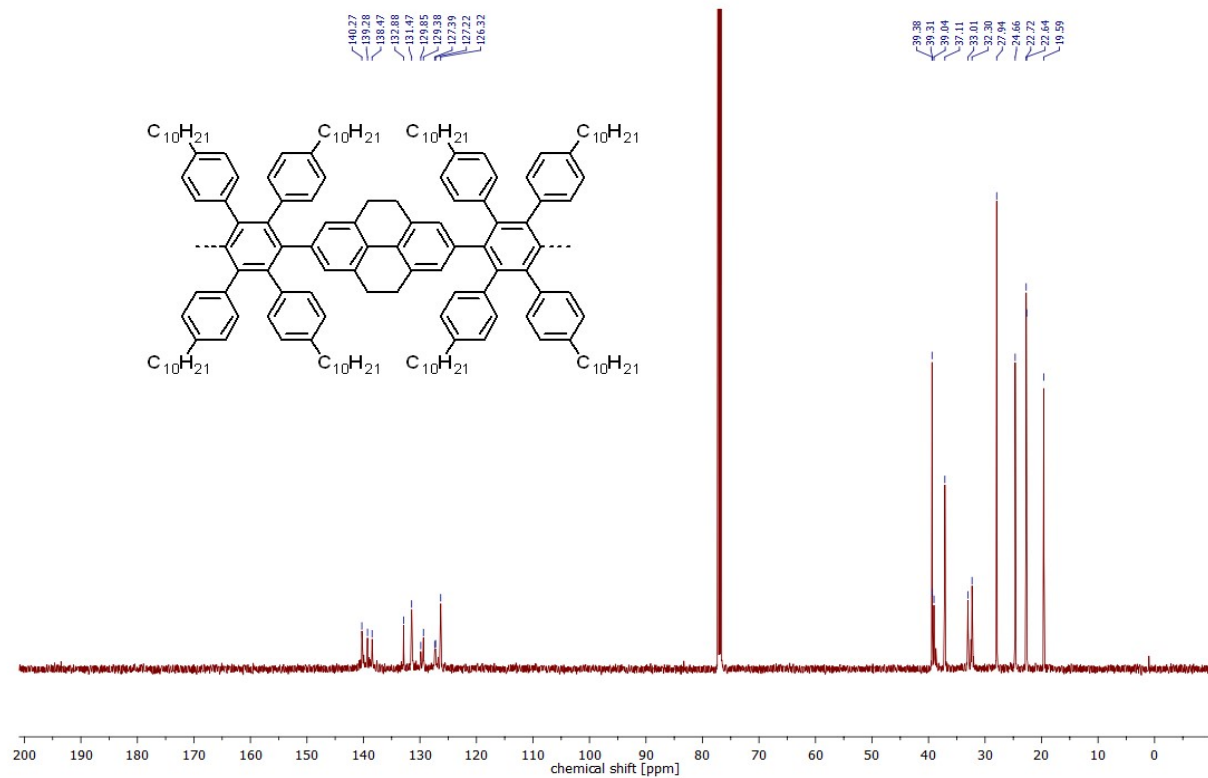

Figure S31. ^{13}C-NMR spectra of polymer **P1** (126 MHz, CDCl$_3$).
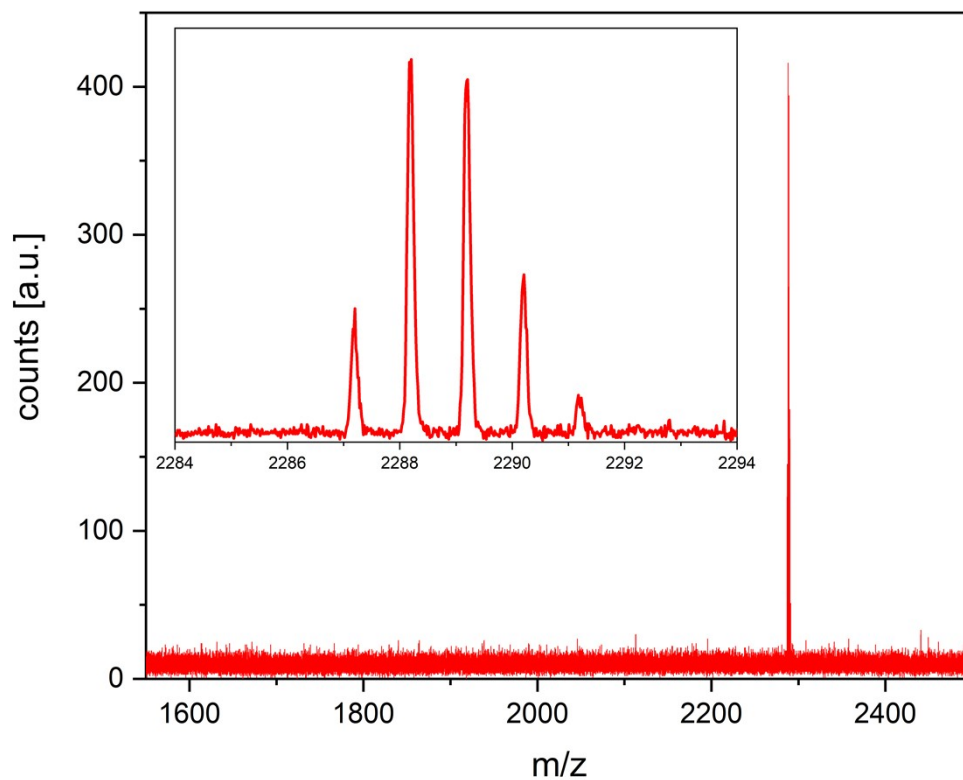
3 MALDI-TOF Spectra

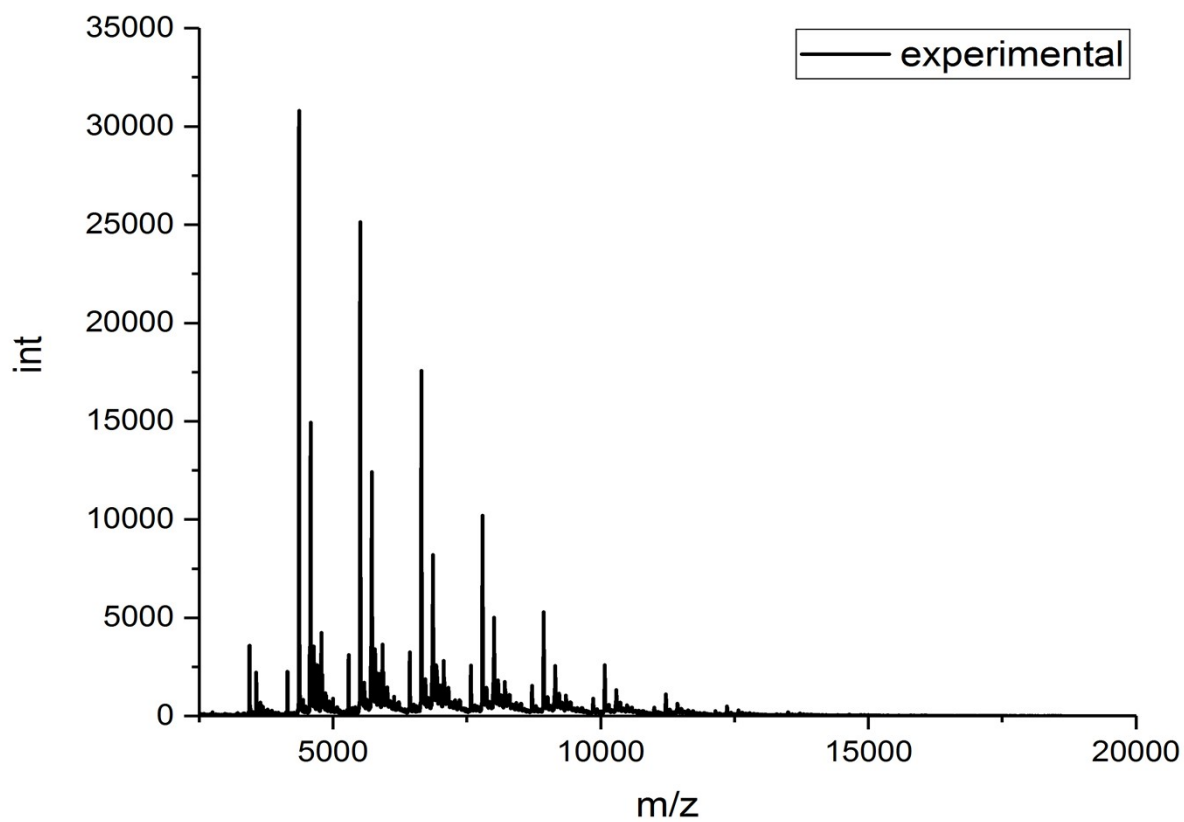**Figure S32.** MALDI-TOF-MS of a partially cyclized compound in the Scholl-reaction towards **1** (DCTB).
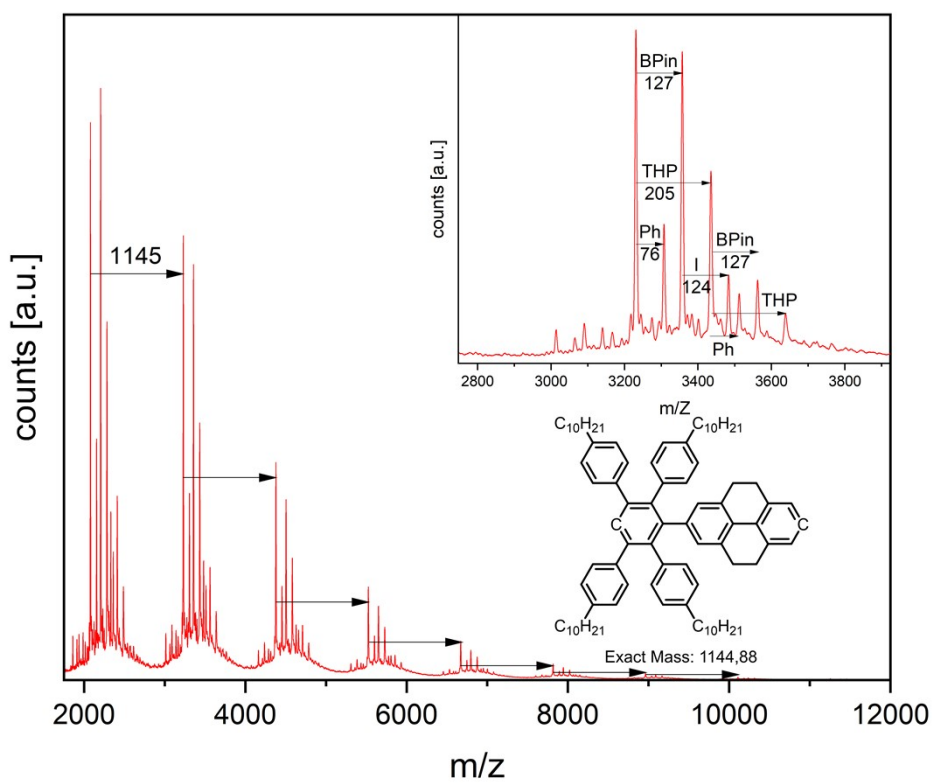
Figure S33. MALDI-TOF-MS of **P1** (linear mode, DCTB, THP = 4,5,9,10-tetrahydropyrene).

Figure S34. MALDI-TOF of insoluble Pyrene containing oligomers.

4 Photoluminescence spectra of 1

Figure S35. Photoluminescence spectra of compound **1**.

Remark to UVVIS of compound **1**: According to the TD-DFT experiments, these absorptions are mainly caused by HOMO→LUMO, HOMO-1→LUMO, HOMO→LUMO+1 and HOMO-1→LUMO+1 transitions. **1** exhibits a maximum and a shoulder in the emission spectra at 579 nm and 622 nm, respectively (ESI Figure **S34**).

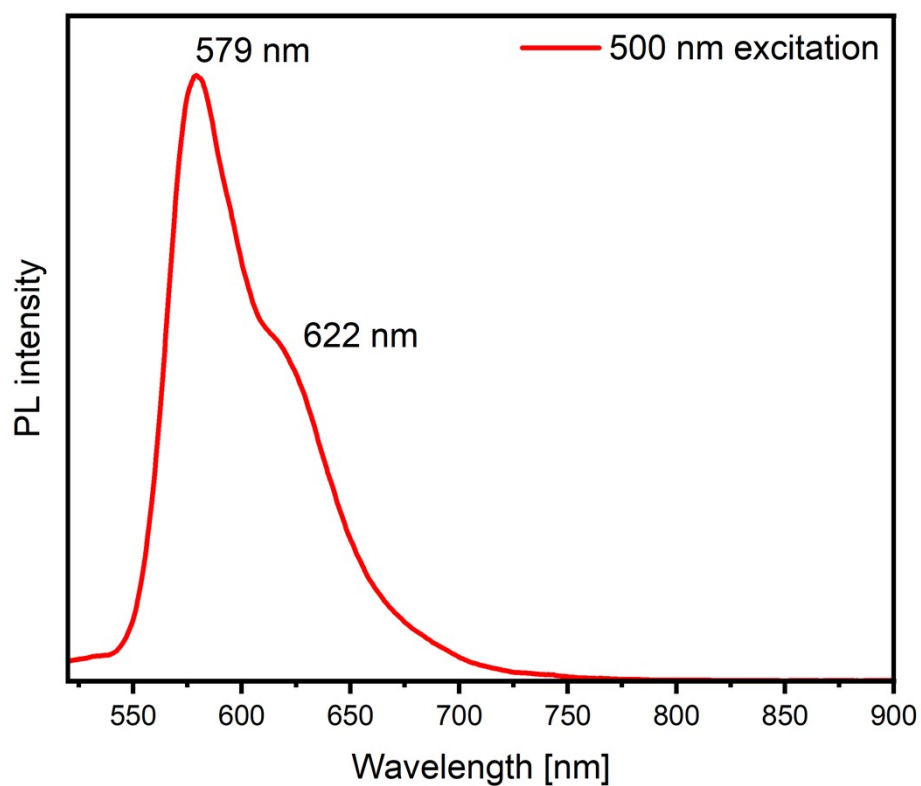# 5 Analytical Gel Permeation Chromatography (GPC) of P1

After fractionating the crude Polymer **P1** in 4 fractions by preparative recycling GPC, the fractions were reinjected into an analytical GPC-device to determine their relative molecular mass distributions against polystyrene standards. Fraction 4 was not analyzed, as it consisted mostly of oligomers.

Molecular Weight Averages

Peak	Mp	Mn	Mw	Mz	Mz+1	Mv	PD
Peak 1	26192	23572	28862	34323	40746	33457	1.224

Figure S36. Analytical GPC results of **P1**, fraction 1 (~10ω% of the crude polymer mixture).

Molecular Weight Averages

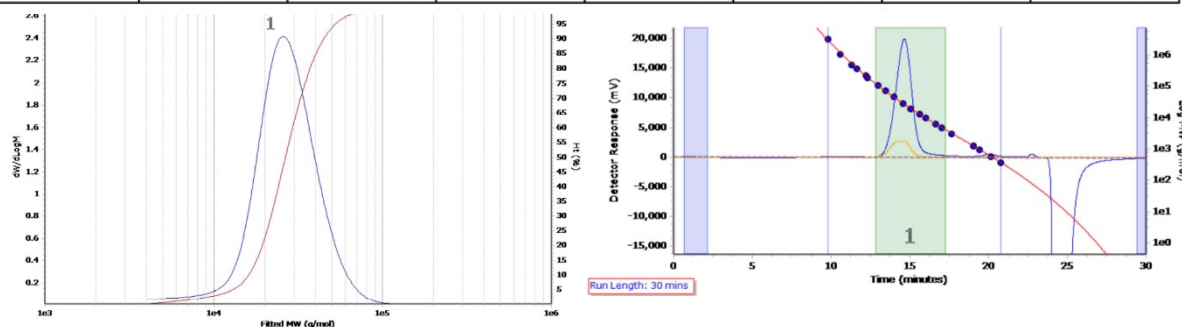| Peak	Mp	Mn	Mw	Mz	Mz+1	Mv	PD
Peak 1	16293	15921	18771	22504	27507	21861	1.179

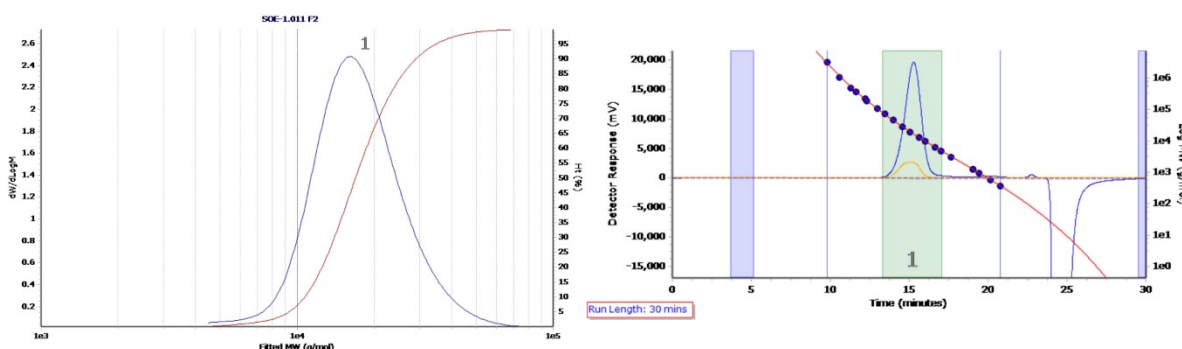**Figure S37.** Analytical GPC results of **P1**, fraction 2 (~22ω% of the crude polymer mixture).

Molecular Weight Averages

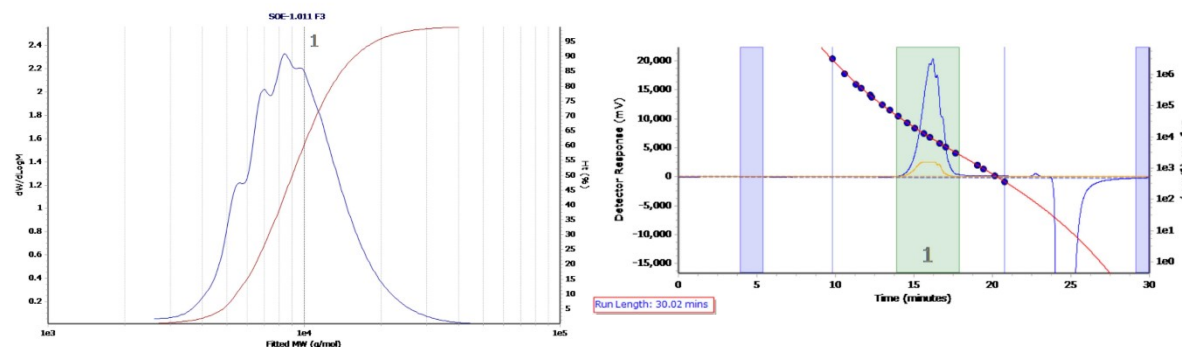| Peak	Mp	Mn	Mw	Mz	Mz+1	Mv	PD
Peak 1	8410	8401	10043	12301	15460	11904	1.195

Figure S38. Analytical GPC results of **P1**, fraction 3 (~37ω% of the crude polymer mixture).

6 X-Ray crystallographic analysis of 11 and 1

Single crystals of compound **11** were obtained by slow evaporation of its dichloromethane solution. Compound **1** crystallized by slow diffusion of Methanol in its CS_2-solution. Suitable single crystals were coated with Paratone-N oil, mounted using a Hampton nylon loop and frozen in the cold nitrogen stream. X-ray diffraction data were collected at 100 K on a Rigaku Oxford Diffraction SuperNova diffractometer using Cu K_α radiation (λ = 1.54184 Å) generated by a micro-focus source. The data reduction and absorption correction were performed using CrysAlis[Pro][3]. For further crystal and data collection details see Tab. S1. The structures were solved using Olex2[4] with the SHELXT package[5] and were refined with SHELXL[5]. Images of the structures were produced with Olex2 software.

The structure of compound **1** was refined using SQUEEZE program of PLATON[6] to account for disordered water molecules in the lattice. Applying SQUEEZE without any solvent modelled resulted in masking 749 electron in the unit cell have been masked accounting for 5 molecules of CS_2 per asymmetric unit. After freely refining two positions of CS_2 the remaining electron density of 500 electrons accounts for 3.3 molecules of CS_2 per asymmetric unit besides the refined 1.3 molecules CS_2.

The structure of compound **11** contains the two conformational enantiomers disordered on the same position. The disorder also effects two of the ortho-substituents. To allow for a convergent refinement, SIMU and SADI restraints were applied on the disordered atoms.

The CIFs for structures reported in this article have been deposited at the Cambridge Crystallographic Data Centre (CCDC) under the deposition numbers 2226715 (for **11**) and 2226716 (for **1**). The data can be obtained free of charge from the CCDC via http://www.ccdc.cam.ac.uk/data_request/cif.

Table S1. Crystallographic Data and reflection collection of compounds **11** and **1**.

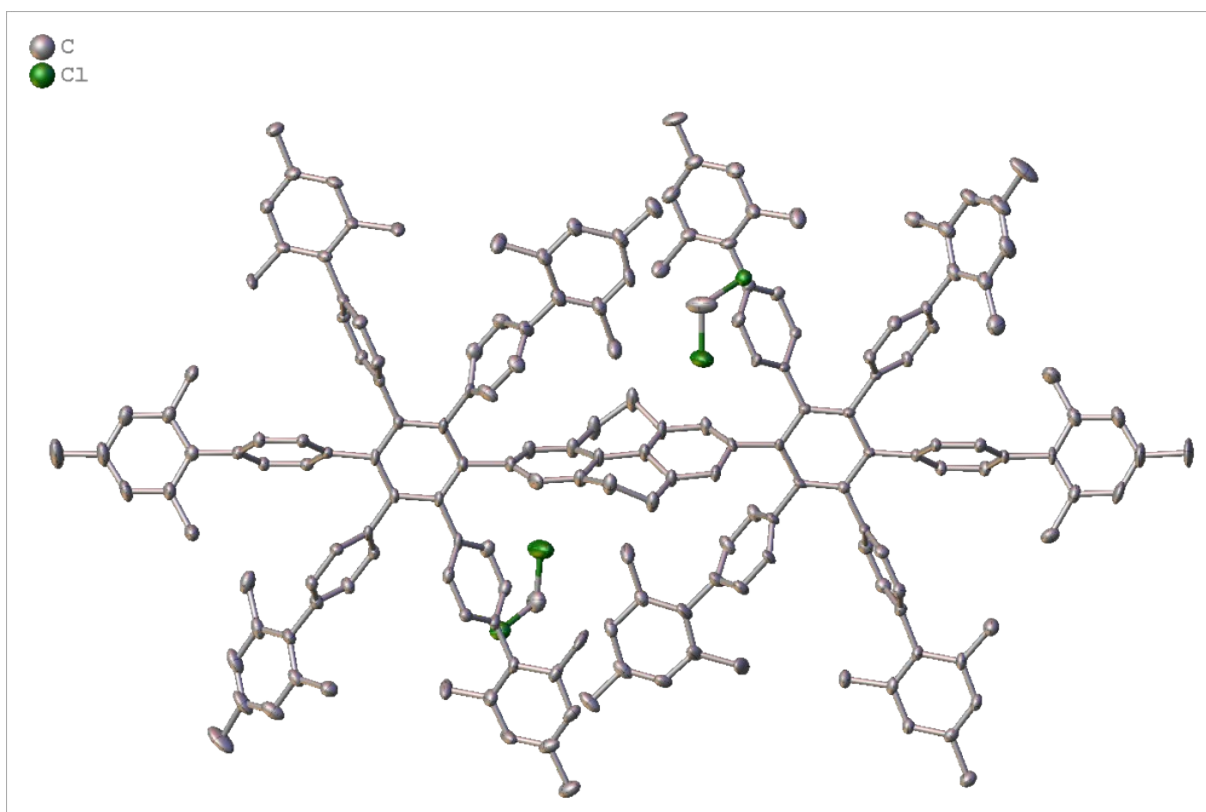|	Compound 11	Compound 1
Empirical formula	$C_{180.23}H_{165.95}Cl_{4.45}$	$C_{183}H_{134}S_{10}$
Formula weight	2489.58	2653.49
Temperature/K	100.00(10)	100.00(10)
Crystal system	triclinic	monoclinic
Space group	$P1$	$P2_1/c$
a/Å	9.72613(10)	23.6811(6)
b/Å	19.54803(19)	28.4303(9)
c/Å	20.00438(18)	21.9446(4)
α/°	75.8276(8)	90
β/°	76.6215(9)	101.217(2)
γ/°	89.2410(8)	90
Volume/Å^3	3583.73(6)	14492.2(7)
Z	1	4
ρ_{calc}g/cm^3	1.154	1.216
μ/mm^{-1}	1.230	1.828
F(000)	1323.0	5568.0
Crystal size/mm^3	0.187 × 0.111 × 0.07	0.173 × 0.09 × 0.051
Radiation	Cu Kα (λ = 1.54184)	Cu Kα (λ = 1.54184)
2Θ range for data collection/°	4.668 to 153.264	4.912 to 134.16
Index ranges	-12 ≤ h ≤ 11, -24 ≤ k ≤ 17, -25 ≤ l ≤ 25	-28 ≤ h ≤ 27, -33 ≤ k ≤ 33, -26 ≤ l ≤ 24
Reflections collected	43621	112827
Independent reflections	19636 [R_{int} = 0.0258, R_{sigma} = 0.0334]	25693 [R_{int} = 0.0908, R_{sigma} = 0.0673]
Data/restraints/parameters	19636/902/1968	25693/4/1689
Goodness-of-fit on F^2	1.034	1.023
Final R indexes [I>=2σ (I)]	R_1 = 0.0459, wR_2 = 0.1216	R_1 = 0.0902, wR_2 = 0.2334
Final R indexes [all data]	R_1 = 0.0548, wR_2 = 0.1317	R_1 = 0.1636, wR_2 = 0.2928
Largest diff. peak/hole / e Å^{-3}	0.39/-0.36	0.72/-0.41
CCDC number	2226715	2226716

Figure S39. Molecular structure of compound **11**, hydrogen atoms and disorder omitted for clarity.
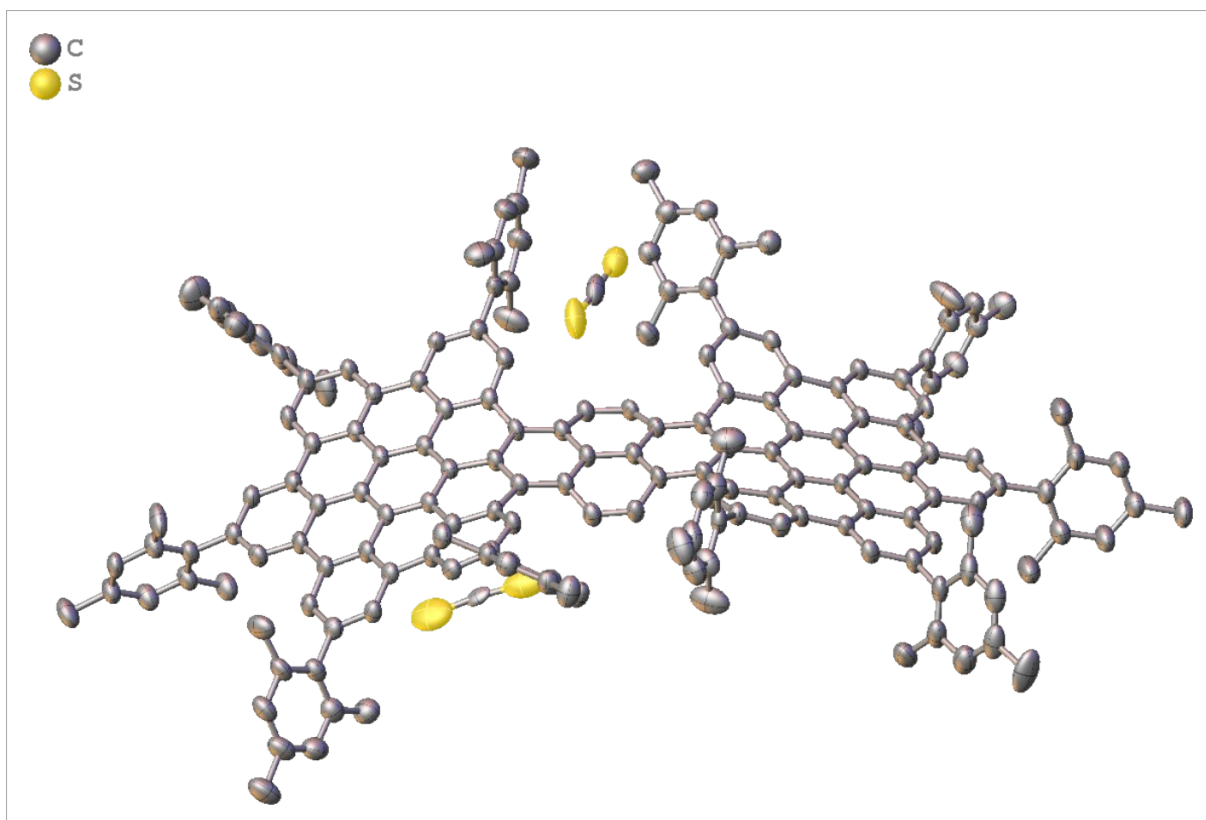

Figure S40. Molecular structure of compound **1**, hydrogen atoms omitted for clarity.
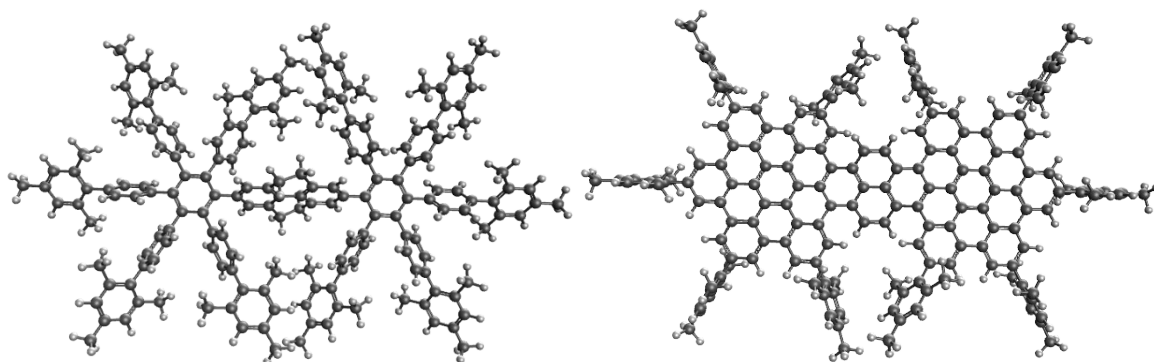
7 DFT Calculation Details

Figure S41. DFT-optimized structure of **11** (left) and **1** (right) on an HSE/6-31G(d) level of theory.
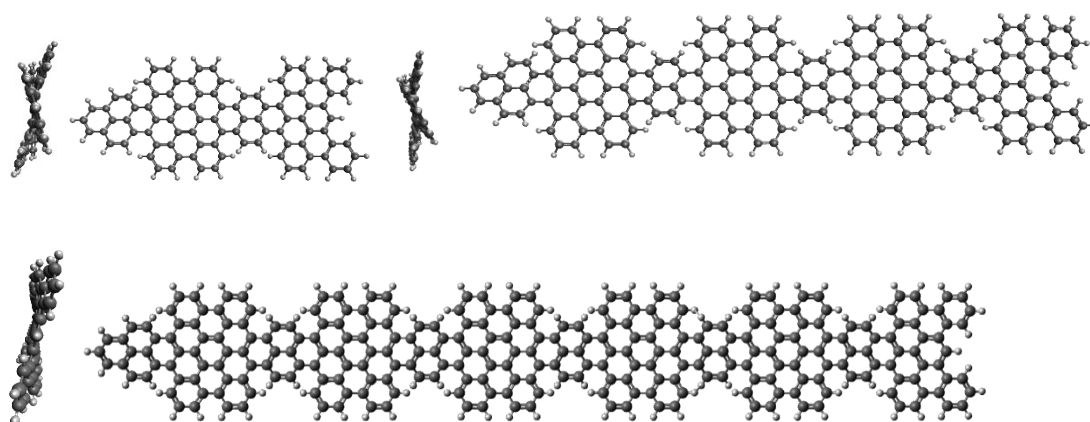

Figure S42. DFT-optimized structure of a **PyGNR** dimer, tetramer, and hexamer on an HSE/6-31G(d) level of theory. The aliphatic side chains were not considered due to negligible impact on the structure. The twist between the two parts of **PyGNR** is of 28.5° for the monomer while it raises to 31° for the other oligomers. For the sake of consistency, the twist of 31° has been considered to build the polymer.
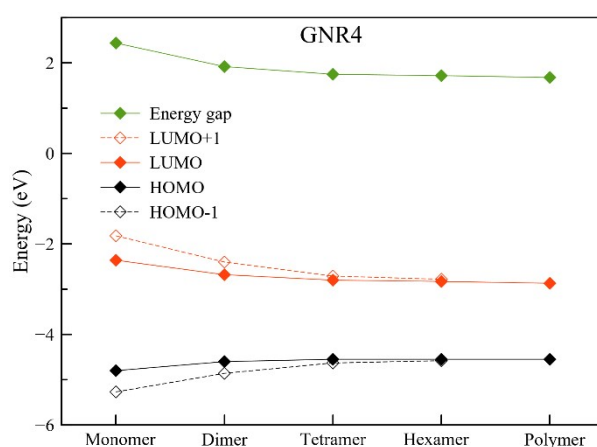

Figure S43. Electronic structure of **PyGNR** oligomers. The energy gap remains almost constant with increasing oligomer length already from the tetramer (1.75 eV) and converges to a value of 1.72 eV for the hexamer, while for the polymer a value of 1.75 eV has been obtained.
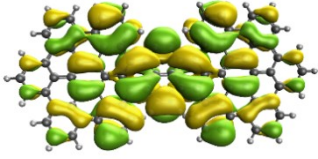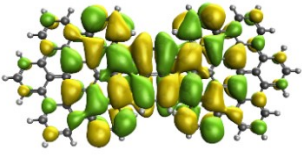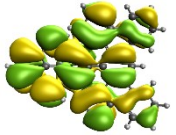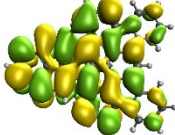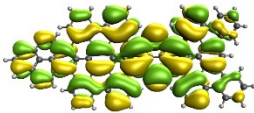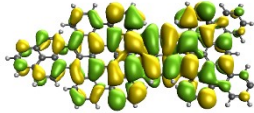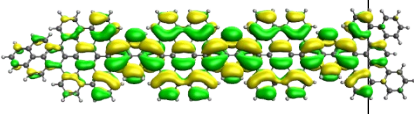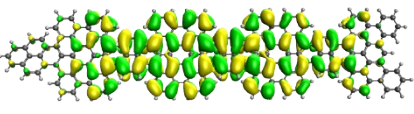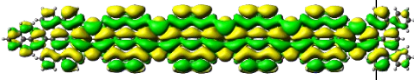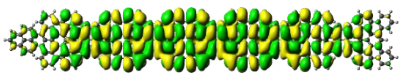
	HOMO	LUMO
Compound 1		
PyGNR Monomer		
PyGNR Dimer		
PyGNR Tetramer		
PyGNR Hexamer		

Table S1. Frontier orbitals of the simulated compounds.
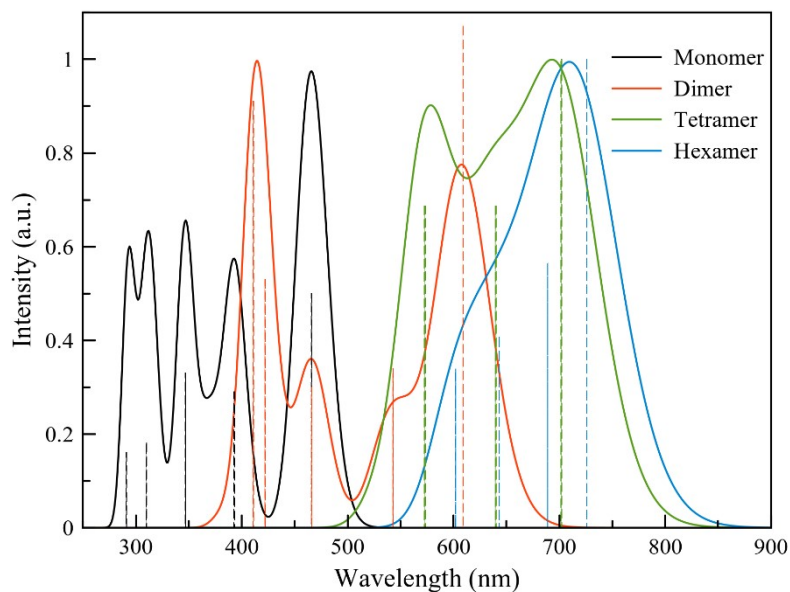
Figure S44. Simulated absorption spectra for **PyGNR** oligomers.

Table S2. Higher energy transitions of the **PyGNR** oligomers. The lowest energy transition state corresponds to a HOMO-LUMO transition for all oligomers.

Monomer ES	Energy (o.s.)	transition	Dimer ES	Energy (o.s.)	transition
1	466 (0.50)	H → L	1	609 (1.07)	H → L
3	393 (0.29)	H-1 → L / H → L+1	3	543 (0.34)	H-1 → L / H → L+1
7	437 (0.33)	H-1 → L+1	7	466 (0.30)	H-1 → L+1
14	310 (0.18)	H-4 → L / H → L+4	12	422 (0.53)	H-2 → L+2
20	291 (0.16)	H-1 → L+4	14	411 (0.91)	H-2 → L+2
Tetramer ES	**Energy (o.s.)**	**transition**	**Hexamer ES**	**Energy (o.s.)**	**transition**
1	702 (1.82)	H → L	1	726 (2.78)	H → L
5	640 (1.25)	H-1 → L+1	4	689 (1.57)	H-1 → L+1
11	573 (1.25)	H-2 → L+2	12	643 (1.13)	H-2 → L+2
			20	602 (0.94)	H-3 → L+3

Figure S45. Band dispersion of **PyGNR**. The dispersion of both VB and CB are moderate, with quite flat bands in the proximity of the Gamma point. This leads to a band gap of 1.75 eV and high values of reduced masses, namely 1.06 m_h and 1.15 m_e.

8   Terahertz spectroscopy

Terahertz (THz) spectroscopy is driven by a commercial Ti:sapphire femtosecond laser system, with repetition rate of 1 KHz and a central wavelength of 800 nm (~50 fs duration). For THz spectroscopy, THz electric field is generated by a zinc telluride (ZnTe) crystal by optical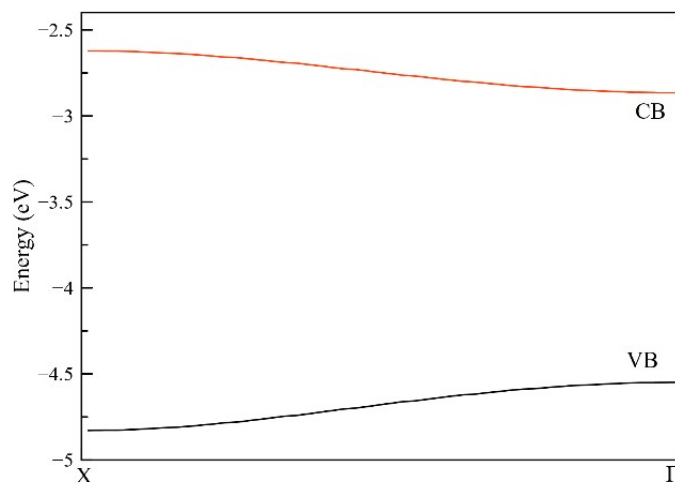 rectification, and probed by a second ZnTe detection crystal by electro-optic method. During the measurement, the entire THz set-up is kept within dry nitrogen atmosphere for avoiding THz absorption from water vapor. For optical pump-THz probe measurement, the photoconductivity can be monitored by charactering the differential transmission of terahertz signal, following: $\Delta\sigma \propto -\Delta E = -(E_{pump} - E_0)$, where E_{pump} and E_0 represent the peak intensity of transmitted THz field with and without photoexcitation (see data in **Figure 5b**).[7,8]

For time-domain THz spectra measurement, we extract the frequency-resolved photoconductivity of GNRs dispersion by using Fourier transformation (see data in **Figure 5c**). In our measurement geometry, the THz electric field travels from air into the front cuvette window, the solvent, and then the back of the cuvette window and back into air. The complex photoconductivity $\Delta\sigma(\omega)$ follows:[7,9,10]

$$\Delta\sigma(\omega) = \left(n^2 - (1 - \Delta\hat{n}(\omega))^2\right)\frac{i\omega}{Z_0 c}, \text{ with } \quad \Delta\hat{n}(\omega) = \left(\frac{1}{n}\frac{n_w - n}{n_w + n} + i\frac{\omega d}{c}\right) - 1\frac{\Delta E(\omega)}{E}$$

where ω, d, and c represent the angular frequency, excitation thickness, and the speed of light in vacuum. n and n_w are the real refractive indices of the solvent and cuvette.

The phenomenological Drude−Smith (DS) model is applied to describe the frequency-resolved complex conductivity (see data in **Figure 5c**).[10,11] The DS model considers the charge scattering occurring not randomly via preferential through backscattering due to, *e.g.*, conjugation or structural deformation in materials. A parameter *c* is introduced to characterize the backscattering probability, ranging from 0 (isotropic scattering) and −1 (100% backscattering). DS model equation reads as:

$$\sigma(\omega) = \frac{\varepsilon_0 \omega_p^2 \tau}{1 - i\omega\tau}\left(1 + \frac{c}{1 - i\omega\tau}\right), \text{ with } \omega_p^2 = \frac{e^2 N}{\varepsilon_0 m^*}$$

where τ, ω_P, ε_0, *e*, *m**, and *c* are the effective carrier momentum scattering time, plasma frequency, vacuum permittivity, elementary charge, charge effective mass, and backscattering rate respectively.

9 Solid state NMR

Solid-state NMR spectra were collected on a Bruker Avance Neo 500 spectrometer equipped with a magnet operating at 11.74 T ($v_L(^1H)$ = 500.39 MHz, $v_L(^{13}C)$ = 125.85 MHz) using a commercial Bruker 1.3 mm DVT H/F/X/Y probe equipped with magic angle gradient coils. Both samples were packed in 1.3 mm o.d. ZrO_2 rotors with Vespel caps. The samples were confined to the central third of the rotor with PTFE tape. The magic angle was calibrated using the sideband pattern of the ^{23}Na spectrum of $NaNO_3$. The 90° pulse lengths of 2 µs for ^1H ($v_{nut}(^1H)$ = 125 kHz) and 5 µs for ^{13}C ($v_{nut}(^{13}C)$ = 50 kHz), respectively, were calibrated using adamantane. The chemical shift scales are given relative to adamantane ($\delta(^1H)$ = 1.85 ppm, $\delta(^{13}C)$ = 29.47 ppm for the highfield signal). Both samples were spun at the magic angle with 62.5 kHz at ambient temperature. Low-power CW decoupling from ^1H with 20 kHz r.f. power was applied while recording the $^{13}C\{^1H\}$ MAS NMR spectra. Recording the 2D ^1H-^1H DQ/SQ spectra employed the BaBaXY16 DQ excitation scheme with 4 rotor periods (64 µs) of excitation. All data processing was performed in TopSpin 4.0.7 and home-written Python scripts.
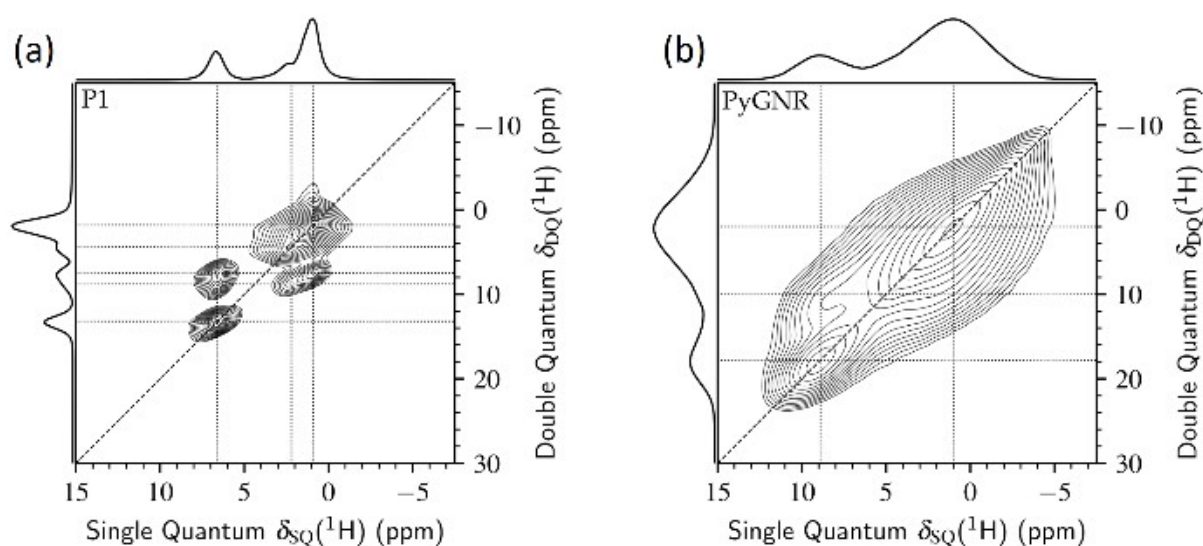

Figure S46. 2D 1H-1H double-quantum/single-quantum NMR (DQ/SQ NMR) for **P1** and **PyGNR**: This technique correlates the spin's chemical shift to the frequency of double quanta that are generated by the direct dipole-dipole interaction.

Additional remarks:

Figure S45a,b) The spatial proximity of protons was probed by 2D ^{1}H-^{1}H double-quantum/single-quantum NMR (DQ/SQ NMR, Figure S45a, b). Similar to the one-dimensional ^{1}H spectrum, the DQ/SQ spectrum of **P1** (Figure S45a) shows sharp correlation signals. Also, correlation of the side chain protons to the aromatic protons is visible. The resolution allows for the identification of another species with a chemical shift of 2.2 ppm that can be assigned to the methylene protons of the tetrahydropyrene unit as they show a correlation to the neighboring aromatic protons at $\delta_{SQ}/\delta_{DQ} \approx$ 2.2 ppm/8.8 ppm and 6.6 ppm/8.8 ppm. Additionally, For **PyGNR**, a DQ/SQ spectrum with two broad signals with a range of chemical shift from −3 ppm to 6 ppm and 6.5 ppm to 11.6 ppm, respectively, is observed (Figure S45b). The significantly lower line width of the aromatic proton signal compared to a previously discussed GNR can be attributed to weaker currents induced in the aromatic core.[12]

Figure 4b) The higher intensity of the aromatic ^{13}C signals centered around 130 ppm of **PyGNR** compared to **P1** is the result of shorter T_1(^{13}C) relaxation times in GNRs as has been observed before.[13] These signals are assigned to quarternary C carbons (140 ppm) in the center and CH carbons (130 ppm) at the edges of the graphene ribbon.[12]

10 IR-Spectra

P1: In the FT-IR spectra (Figure 4c), **P1** exhibits typical aromatic CH-stretching (dark purple) around 3060-3020 cm^{-1}, followed by three overlapping aliphatic stretching bands caused by the side chains in the region of 3000-2750 cm^{-1} (light purple). The fingerprint region (900-600 cm^{-1}) contains various out of plane CH-wagging vibrations characteristic of the polymer. To assist in the identification of the corresponding vibrations, DFT calculations on the HSE/6-31G(d) level of theory were performed. In this region, the peak at 885 cm^{-1} can be attributed to the SOLO-mode (CH-wagging of an aromatic proton without adjacent protons, orange)[14] of the tetrahydropyrene moiety. The broad peak in the region of 850-790 cm^{-1} (yellow) was predicted to arise from a combination of the DUO-waggings (CH-wagging of an aromatic proton with one adjacent proton)[14] of the polyphenylene and the sp^3-CH$_2$ bending of the tetrahydropyrene moieties. Lower energy vibrations correspond to various aromatic and aliphatic CH and CC bending modes.

PyGNR: The olive green peaks at 741 cm^{-1} can be attributed aliphatic wagging vibrations from the solubilizing 3,7-dimethyloctyl chains.

11 SEM and EDX results

Scanning electron microscopy (SEM) was performed on a Zeiss Gemini 500 microscope equipped with an EDX detector. The powder samples were deposited on Si substrate for the measurement.
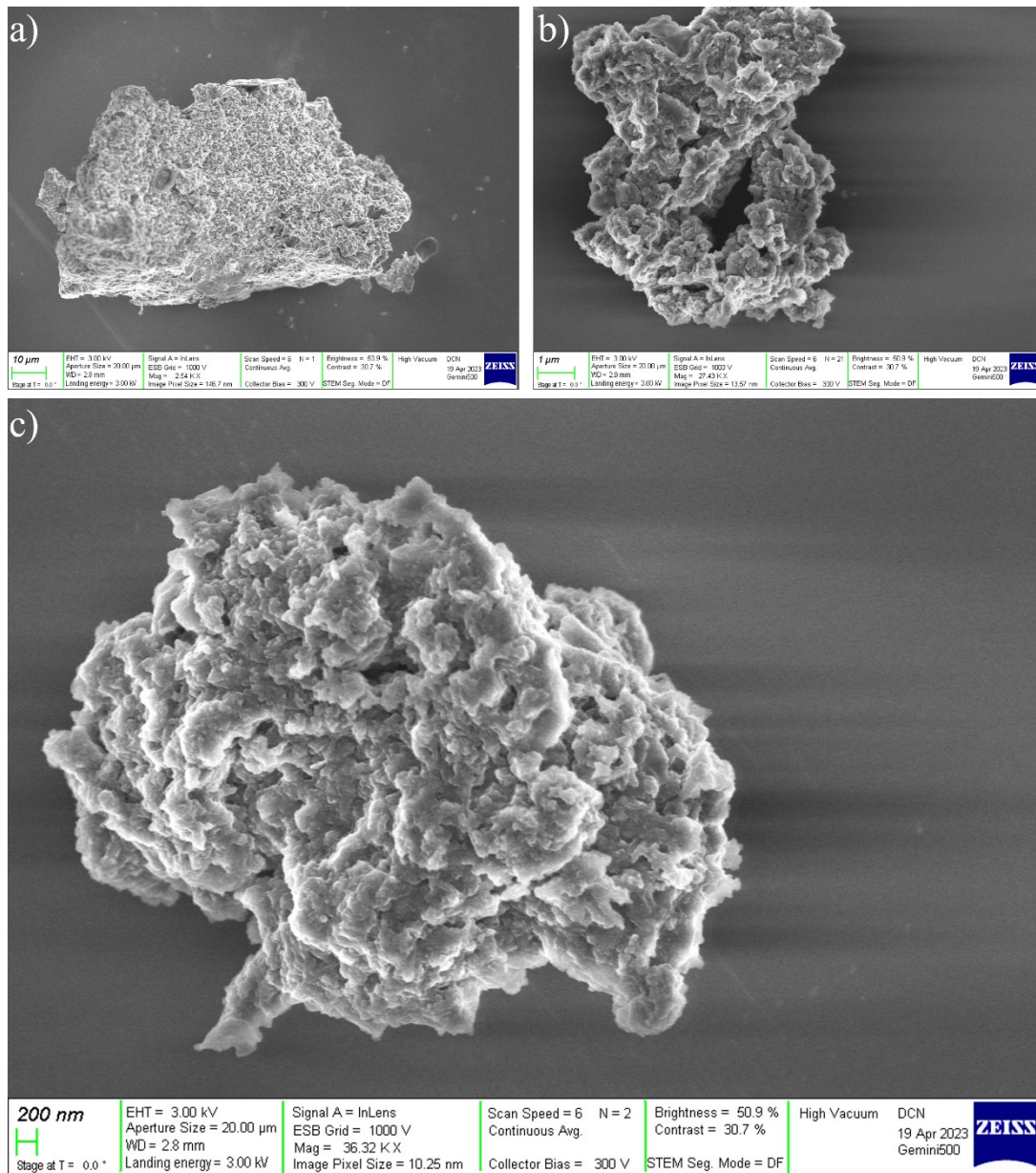

Figure S47. SEM images of **PyGNR** at different magnifications; a) 2.54k-times; b) 27.43k-times; c) 36.32k-times.
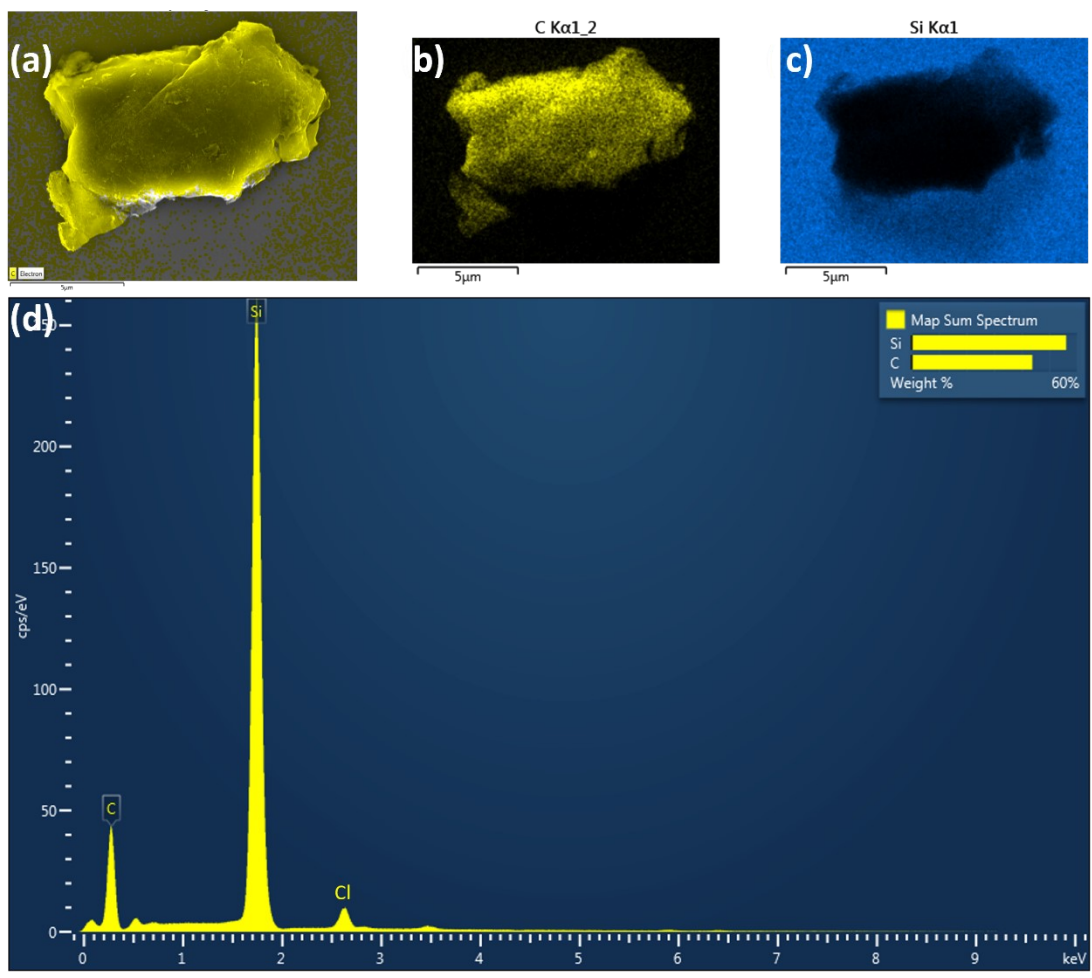
Figure S48. EDX investigation of **PyGNR** (scalebars 5 μm); a) layered image; b) colorized for carbon; c) colorized for silicon (substrate); d) EDX-spectra; iron Kα would be expected ~ 6.4 keV.

12 TEM imaging

TEM was conducted using JEOL JEM F200 operated at 200 kV acceleration voltage equipped with a GATAN OneView CMOS camera for fast imaging.
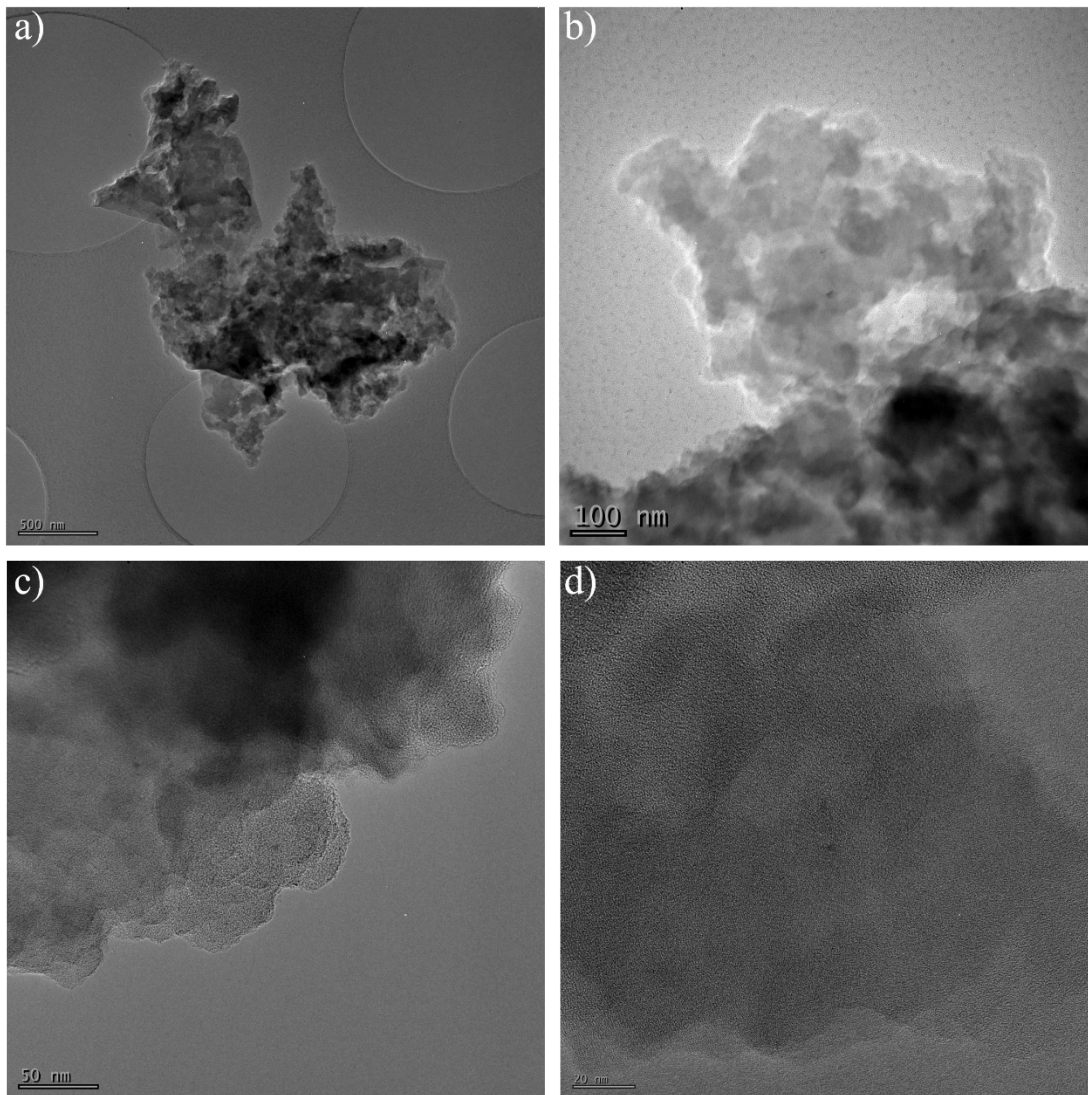

Figure S49. TEM images of **PyGNR** at different magnifications; a) 15k-times; b) 50k-times; c) 150k times; d) 300k-times.

13 Powder-XRD

The diffractogram was measured with a STOE Stadi P XRD equipped with a copper X-ray tube. The power values were 40 mA and 40 kV. Scans were accumulated over one hour in transmission mode.
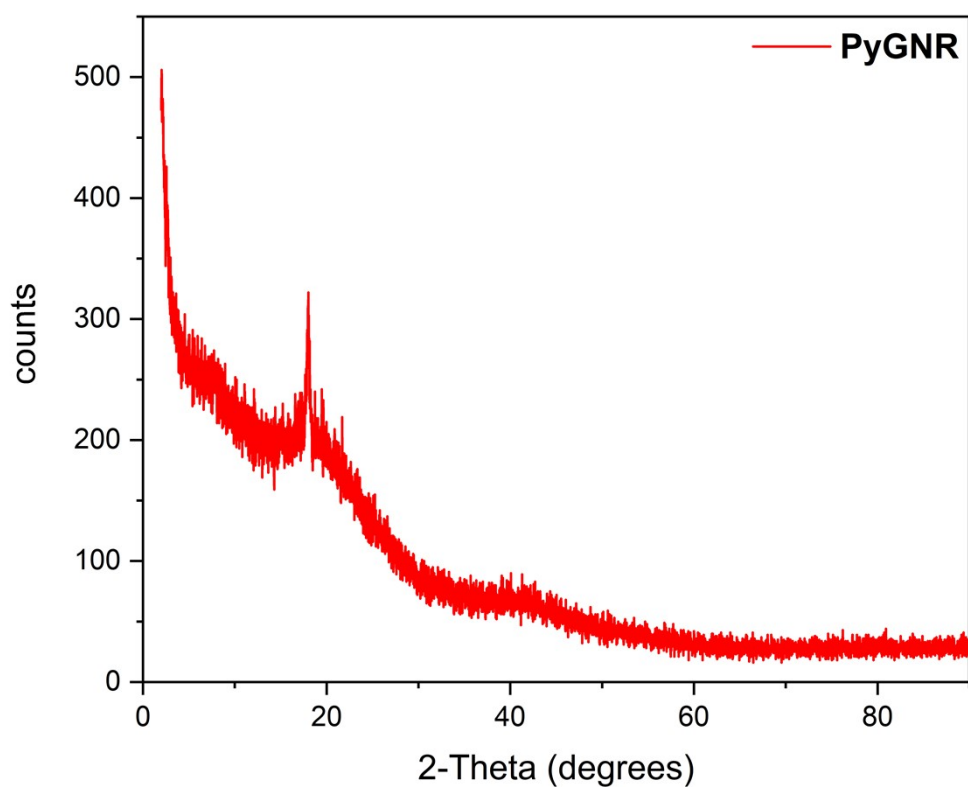

Figure S50. PXRD of **PyGNR**, indicating an amorphous structure.

14 Solid/liquid STM measurements

STM-characterization: Scanning tunneling microscopy experiments were performed using a Molecular Imaging (Agilent Tech.) operating at constant current mode at room temperature. Mechanically cut Pt/Ir wire (80/20, diameter 0.25 mm, Advanced Research Materials) was used as the tip. Experimental STM parameters (U_{bias} and I_{set}) correspond to the substrate bias and the tunneling current respectively and are indicated in every figure. Calibration was performed using software Scanning Probe Image Processor (SPIP, Image Metrology). The HOPG substrate (grade ZYB Momentive Performance Material Quartz Inc., Strongsville, OH, USA) was freshly cleaved using scotch tape prior to every experiment. Heptanoic acid was used as received from Merck. The molecular models were built using HyperChem™ software (version 8.0.1).

Sample preparation: The HOPG substrate (grade ZYB Momentive Performance Material Quartz Inc., Strongsville, OH, USA) was freshly cleaved using scotch tape prior to every experiment. After this, pure heptanoic acid was dropcasted as received from Merck. Afterwards, a tiny amount of Py-GNR powder was introduced on top of the HOPG surface and in complete contact with the heptanoic acid. After some minutes, the STM imaging was carried out.
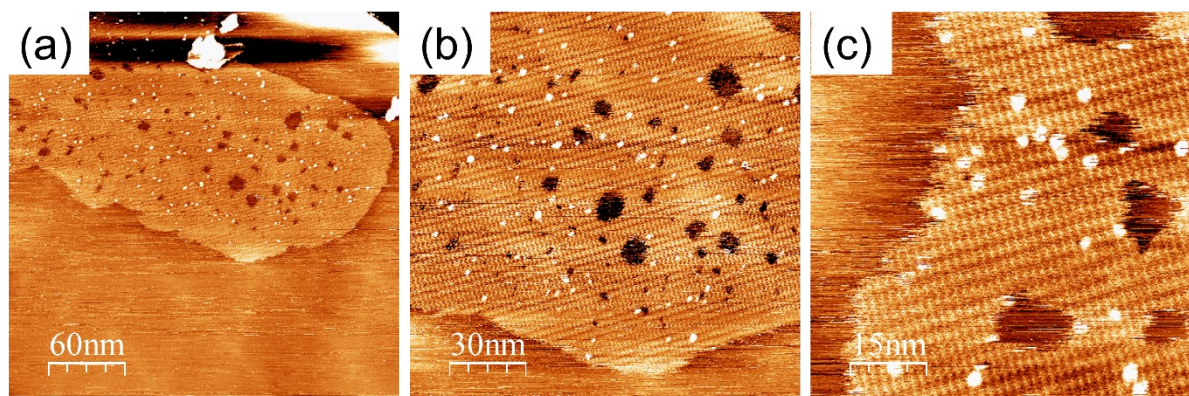

Figure S51. (a-c) STM images obtained for **PyGNR**, self-assembled, showing a clear striped structure at the heptanoic acid/HOPG interface. U_{bias}= -0.4 V and I_{set} = 0.05 nA.

15 TGA of PyGNR

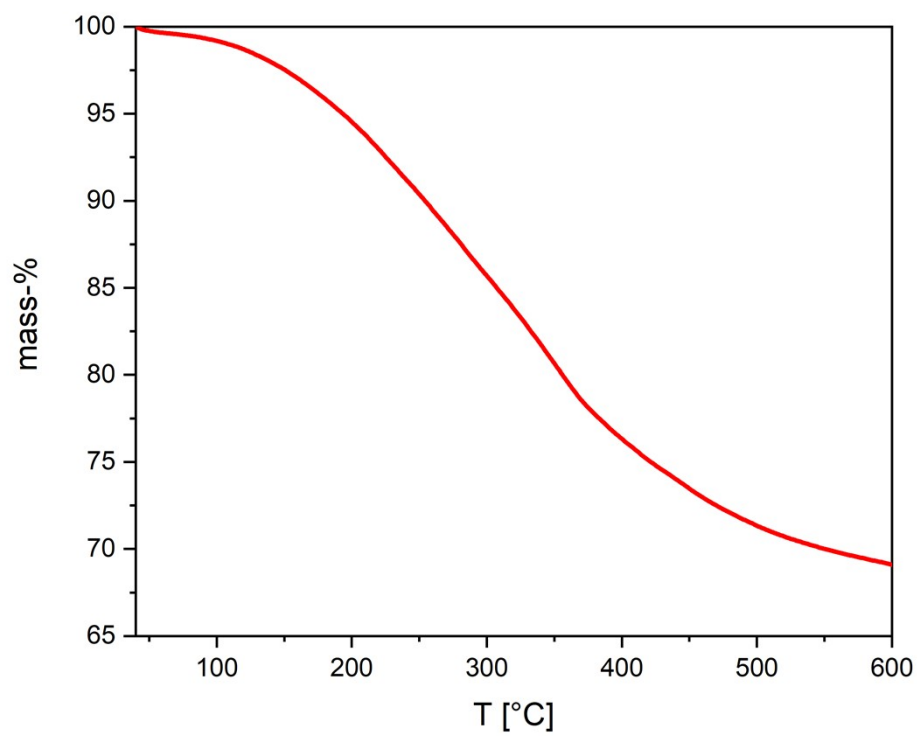TGA was carried out on a STA 449 F5 "Jupiter" from Netzsch at a heating rate of 5 K/min under Argon.

Figure S52. TGA of **PyGNR**.

17 References

[1]   National Institute of Advanced Industrial Science and Technology (AIST), "SDBS No.: 1868," **1999**.

[2]   National Institute of Advanced Industrial Science and Technology (AIST), "SDBS No.: 878," **1999**.

[3]   Crysalis Pro Software System, Rigaku Corporation, Wroclaw, Poland **2022**.

[4]   O. v. Dolomanov, L. J. Bourhis, R. J. Gildea, J. A. K. Howard, H. Puschmann, *J. Appl. Crystallogr.,* 2009, **42**, 339–341.

[5]   G. M. Sheldrick, *Acta Crystallogr., Sect. A: Found. Adv.,* 2015, **71**, 3–8.

[6]   A. L. Spek, *Acta Crystallogr., Sect. C: Struct. Chem.,* 2015, **71**, 9–18.

[7]   R. Ulbricht, E. Hendry, J. Shan, T. F. Heinz, M. Bonn, *Rev. Mod. Phys.,* 2011, **83**, 543–586.

[8]   W. Zheng, N. F. Zorn, M. Bonn, J. Zaumseil, H. I. Wang, *ACS Nano,* 2022, **16**, 9401–9409.

[9]   J. D. Jackson, *Classical Electrodynamics*, Wiley, New York, **1975**.

[10]   S. A. Jensen, R. Ulbricht, A. Narita, X. Feng, K. Müllen, T. Hertel, D. Turchinovich, M. Bonn, *Nano Lett.,* 2013, **13**, 5925–5930.

[11]   T. L. Cocker, D. Baillie, M. Buruma, L. v. Titova, R. D. Sydora, F. Marsiglio, F. A. Hegmann, *Phys. Rev. B.,* 2017, **96**, 205439.

[12]   A. Narita, I. A. Verzhbitskiy, W. Frederickx, K. S. Mali, S. A. Jensen, M. R. Hansen, M. Bonn, S. de Feyter, C. Casiraghi, X. Feng, K. Müllen, *ACS Nano,* 2014, **8**, 11622–11630.

[13]   X. Yao, W. Zheng, S. Osella, Z. Qiu, S. Fu, D. Schollmeyer, B. Müller, D. Beljonne, M. Bonn, H. I. Wang, K. Müllen, A. Narita, *J. Am. Chem. Soc.* 2021, **143**, 5654–5658.

[14]   M. Tommasini, A. Lucotti, M. Alfè, A. Ciajolo, G. Zerbi, *Spectrochim. Acta, Part A,* 2016, **152**, 134–148.